

การเตรียมและการวิเคราะห์สมบัติของพอลิเบนซอกซาซีนที่ดัดแปรด้วยสารไดแอนไฮไดรด์ที่มี
ฟลูออรีนเป็นองค์ประกอบ

นายพัชรรัตน์ ภัทรสิริวงศ์



จุฬาลงกรณ์มหาวิทยาลัย
CHULALONGKORN UNIVERSITY

บทคัดย่อและแฟ้มข้อมูลฉบับเต็มของวิทยานิพนธ์ตั้งแต่ปีการศึกษา 2554 ที่ให้บริการในคลังปัญญาจุฬาฯ (CUIR)

เป็นแฟ้มข้อมูลของนิสิตเจ้าของวิทยานิพนธ์ ที่ส่งผ่านทางบัณฑิตวิทยาลัย

วิทยานิพนธ์นี้เป็นส่วนหนึ่งของการศึกษาตามหลักสูตรปริญญาวิศวกรรมศาสตรมหาบัณฑิต
The abstract and full text of theses from the academic year 2011 in Chulalongkorn University Intellectual Repository (CUIR)

สาขาวิชาวิศวกรรมเคมี, ภาควิชาวิศวกรรมเคมี
are the thesis authors' files submitted through the University Graduate School.

คณะวิศวกรรมศาสตร์ จุฬาลงกรณ์มหาวิทยาลัย

ปีการศึกษา 2558

ลิขสิทธิ์ของจุฬาลงกรณ์มหาวิทยาลัย

Preparation and Characterization of Fluorine-Containing Dianhydride-Modified
Polybenzoxazine

Mr. Patcharat Pattharasiriwong



A Thesis Submitted in Partial Fulfillment of the Requirements
for the Degree of Master of Engineering Program in Chemical Engineering

Department of Chemical Engineering

Faculty of Engineering

Chulalongkorn University

Academic Year 2015

Copyright of Chulalongkorn University

Thesis Title	Preparation and Characterization of Fluorine-Containing Dianhydride-Modified Polybenzoxazine
By	Mr. Patcharat Pattharasiriwong
Field of Study	Chemical Engineering
Thesis Advisor	Associate Professor Sarawut Rimdusit, Ph.D.

Accepted by the Faculty of Engineering, Chulalongkorn University in Partial Fulfillment of the Requirements for the Master's Degree

..... Dean of the Faculty of Engineering
(Professor Bundhit Eua-arporn, Ph.D.)

THESIS COMMITTEE

..... Chairman
(Associate Professor Siriporn Damrongsakkul, Ph.D.)

..... Thesis Advisor
(Associate Professor Sarawut Rimdusit, Ph.D.)

..... Examiner
(Associate Professor Artiwan Shotipruk, Ph.D.)

..... External Examiner
(Associate Professor Chirakarn Muangnapoh, Dr.Ing.)

5670300721 : MAJOR CHEMICAL ENGINEERING

KEYWORDS: POLYBENZOXAZINE / FLUORINE-CONTAINING POLYMER / DIANHYDRIDE / POLYMER ALLOY

PATCHARAT PATTHARASIRIWONG: Preparation and Characterization of Fluorine-Containing Dianhydride-Modified Polybenzoxazine. ADVISOR: ASSOC. PROF. SARAWUT RIMDUSIT, Ph.D., 92 pp.

In this research, three types of fluorine-containing benzoxazine monomers i.e. BA-4fa, BAF-a and BAF-4fa are successfully prepared via solventless technology and their chemical functionality has been confirmed by fourier transform infrared spectroscopy (FTIR). Fluorine-containing polymer alloy films were fabricated by reacting bisphenol-AF/aniline based polybenzoxazine (PBAF-a) with 4,4'-(hexafluoroisopropylidene)diphthalic anhydride (6FDA) in n,n-dimethylacetamide solvent. From the results, the alloy films show superior degradation temperature at 10% weight loss up to 464°C and significant enhancement in char yield at 800°C with a value up to 56% by weight due to the formation of ester linkage between hydroxyl group of the PBAF-a and the carbonyl group in the dianhydride resulting in a more flexibility in PBAF-a/6FDA. Moreover, glass transition temperature of the alloy films increase with increasing dianhydride content and exhibit a maximum value of 287°C at 2.5/1 PBAF-a/6FDA mole ratio. The incorporation of fluorine groups into polybenzoxazine is able to decrease dielectric constant of the resulting alloys. Additionally, the alloy films also provide a greater hydrophobicity behavior as evidently seen from a higher water contact angle with increasing amount of the 6FDA. Therefore, PBAF-a/6FDA alloy films are appropriate for an application as polymeric film for coating and high thermal resistant material.

Department: Chemical Engineering Student's Signature

Field of Study: Chemical Engineering Advisor's Signature

Academic Year: 2015

ACKNOWLEDGEMENTS

I would like to express my sincere gratitude to my thesis advisor, Assoc. Prof. Dr. Sarawut Rimdusit and Asst. Prof. Dr. Chanchira Jubsilp for precious advice, guidance and support helped me overcome many crisis situations and finish this dissertation. Furthermore, I deeply appreciated all the things. I have learnt from them and for the opportunity to work in their group. I really enjoyed our meeting and pleasure with my thesis.

Besides my advisor, I am great appreciate to the chairman, Assoc. Prof. Dr. Siriporn Damrongsakkul and committee members, Assoc. Prof. Dr. Artiwan Shotipruk and Assoc. Prof. Dr. Chirakarn Muangnapoh for their encouragement, insightful comments, and instructive questions.

In addition, I would like to thanks Warunya Junhom from Mettler Toledo (Thailand) Ltd. for assistance on Thermal Mechanical Analysis (TMA).

This research has been supported by the Ratchadaphiseksomphot Endowment Fund 2013 of Chulalongkorn University (CU-56-909-AM).

Last but not least, I most gratefully acknowledge all members of Polymer Engineering Laboratory of the Department of Chemical Engineering, Faculty of Engineering, Chulalongkorn University, for all their support and care helped me support throughout the period of this research. I greatly value their friendship and I deeply appreciate their belief in me.

Finally, I would like to wholeheartedly give all gratitude to the members of my family, who have been a constant source of love, concern, support and strength during my studies. Also, every person who deserves thanks for encouragement and support that cannot be listed.

CONTENTS

	Page
THAI ABSTRACT.....	iv
ENGLISH ABSTRACT	v
ACKNOWLEDGEMENTS	vi
CONTENTS.....	vii
LIST OF TABLES.....	x
LIST OF FIGURES	xii
CHAPTER I INTRODUCTION	1
1.1 Overview.....	1
1.2 Objectives	7
1.3 Scopes of research	7
CHAPTER II THEORY	9
2.1 Benzoxazine resin	9
2.2 Fluorine – containing polymers	10
2.3 Bisphenol-A	12
2.4 Bisphenol-AF.....	14
2.5 Formaldehyde	15
2.6 Aniline	17
2.7 4-(trifluoromethyl)aniline	18
2.8 Anhydride	19
2.9 N,N-Dimethylacetamide	20
CHAPTER III LITERATURE REVIEWS.....	22
CHAPTER IV EXPERIMENTAL	34

	Page
4.1 Raw materials.....	34
4.2 Synthesis of fluorine-containing benzoxazine monomer	34
4.3 Preparation of the 6FDA based polybenzoxazine alloy films	35
4.4 Characterizations of the 6FDA based polybenzoxazine alloy films	36
4.4.1 Fourier transform infrared spectroscopy (FTIR)	36
4.4.2 Differential scanning calorimetry (DSC).....	36
4.4.3 Dynamic mechanical analysis (DMA).....	36
4.4.4 Thermogravimetric analysis (TGA)	37
4.4.5 Thermal mechanical analysis (TMA)	37
4.4.6 Dielectric constant	37
4.4.7 Radius of curvature (Flexibility of alloy films).....	38
4.4.8 Water contact angle.....	38
4.4.9 Solvent extraction.....	38
CHAPTER V RESULTS AND DISCUSSION	43
5.1 Preparation and characterization of fluorine-containing benzoxazine monomers	43
5.1.1 Preparation of fluorine-containing benzoxazine monomers.	43
5.1.2 Characterizations of fluorine-containing benzoxazine monomers by fourier transform infrared (FTIR) spectroscopy and thermogravimetric analyzer (TGA).....	45
5.2 Preparation and characterization of 6FDA modified polybenzoxazine alloy films 46	
5.2.1 Preparation of 6FDA modified polybenzoxazines alloy films	46

	Page
5.2.2 Characterization of 6FDA modified polybenzoxazines alloy films by using thermogravimetric analyzer (TGA)	47
5.3 Fourier transform infrared spectroscopy (FTIR) study of 6FDA modified PBAF-a alloy films	48
5.4 Differential scanning calorimetry (DSC) study of 6FDA modified PBAF-a alloy films	51
5.5 Dynamic mechanical analyzer (DMA) study of 6FDA modified PBAF-a alloy films	52
5.6 Thermal stability of 6FDA modified PBAF-a alloy films	54
5.7 Thermal mechanical of 6FDA modified PBAF-a alloy films	55
5.8 Dielectric constant of 6FDA modified PBAF-a alloy films	56
5.9 Radius of curvature of 6FDA modified PBAF-a alloy films	57
5.10 Contact angle of 6FDA modified PBAF-a alloy films	58
5.11 Solvent extraction of 6FDA modified PBAF-a alloy films	59
CHAPTER VI	85
CONCLUSIONS	85
REFERENCES	86
VITA	92

LIST OF TABLES

	Page
Table 1.1 Summary of trade names, companies, applications and properties of major fluorine-containing polymers	2
Table 2.1 Applications of fluoropolymers.....	11
Table 2.2 Physical and chemical properties of bisphenol-A.....	13
Table 2.3 Physical and chemical properties of bisphenol-AF.....	15
Table 2.4 Physical and chemical properties of paraformaldehyde	16
Table 2.5 Physical and chemical properties of aniline.....	18
Table 2.6 Physical and chemical properties of 4-(trifluoromethyl)aniline.....	19
Table 2.7 Physical and chemical properties of 4,4'-(hexafluoroisopropylidene) diphthalic anhydride (6FDA)	20
Table 2.8 Physical and chemical properties of n,n-dimethylacetamide (DMAc).....	21
Table 3.1 Properties of copolybenzoxazine	24
Table 3.2 Properties of PBA-a and PBA-alloys with aromatic dianhydrides.....	28
Table 3.3 Contact angle and surface free energy of polyimide films.....	30
Table 3.4 Color coordinates and cutoff wavelength λ_0 from UV-vis spectra of the polyimide films.	33
Table 5.1 Summarize of thermogravimetric analysis data of polybenzoxazine/6FDA alloy films	76
Table 5.2 Glass transition temperature (T_g) of fluorine-containing benzoxazine and their PBAF-a/6FDA alloy films at various mole ratios	77

Table 5.3 Glass transition temperature from loss modulus (E''), storage modulus (E') at room temperature (35°C), storage modulus at rubbery plateau (E') and crosslink density of fluorine-containing benzoxazine and PBAF-a/6FDA alloy films at various mole ratios which were determined by DMA	78
Table 5.4 Degradation temperature at 5% weight loss (T_{d5}), Degradation temperature at 10% weight loss (T_{d10}), residue weight (char yield) at 800°C and LOI of fluorine-containing benzoxazine and PBAF-a/6FDA alloy films at various mole ratios	79
Table 5.5 Glass transition temperature (T_g) from TMA and coefficient of thermal expansion of fluorine-containing benzoxazine and their PBAF-a/6FDA alloy films at various mole ratios	80
Table 5.6 Dielectric constants of fluorine-containing benzoxazine and PBAF/a:6FDA alloy films at various mole ratios	81
Table 5.7 Radius of curvature of PBAF-a/6FDA alloy films at various mole ratios	82
Table 5.8 Contact angle and surface free energy of fluorine-containing benzoxazine and PBAF-a/6FDA alloy films at various mole ratios	83
Table 5.9 Solvent extraction data at various mole ratios of 6FDA modified PBA-a alloy films	84

LIST OF FIGURES

	Page
Figure 1.1 Electronegativity of the elements in the periodic table suggesting fluorine atom into possess the highest value.	2
Figure 2.1 Schematic synthesis of monofunctional benzoxazine monomer.	9
Figure 2.2 Schematic synthesis of bifunctional benzoxazine monomer.	10
Figure 2.3 Bisphenol-A used in benzoxazine synthesis.	13
Figure 2.4 Bisphenol-AF used in benzoxazine synthesis.	14
Figure 2.5 Structure of bisphenol-AF.	14
Figure 2.6 Paraformaldehyde powder used in benzoxazine synthesis.	16
Figure 2.7 Structure of paraformaldehyde.	16
Figure 2.8 Aniline used in benzoxazine synthesis.	17
Figure 2.9 Structure of aniline.	17
Figure 2.10 4-(trifluoromethyl)aniline used in benzoxazine synthesis.	18
Figure 2.11 Structure of 4-(trifluoromethyl)aniline.	18
Figure 2.12 4,4'-(hexafluoroisopropylidene)diphthalic anhydride (6FDA).	19
Figure 2.13 Structure of 4,4'-(hexafluoroisopropylidene)diphthalic anhydride (6FDA).	20
Figure 2.14 N,N-dimethylacetamide.	21
Figure 2.15 Structure of n,n-dimethylacetamide (DMAc).	21
Figure 3.1 Schematic synthesis of fluorine-containing benzoxazine monomer.	23
Figure 3.2 The structure of copolybenzoxazine with PBA-a/PBAF-4fa.	23
Figure 3.3 FTIR spectra of BAF-4fa monomer.	25
Figure 3.4 Structure of the alloy films.	26

	Page
Figure 3.5 FTIR spectra of PBA-a alloy with aromatic dianhydrides: (a) PBA-a: PMDA (b) PBA-a : s-BPDA (c) PBA-a : BTDA.	27
Figure 3.6 Appearance of alloy films: (a) PBA-a, (b) PBA-a alloy with aromatic dianhydrides.	27
Figure 3.7 Yellow index value of polyimides films.	29
Figure 3.8 Structure of polyimides (a) fluorine-containing polyimide (b) non-fluorine-containing polyimide.	29
Figure 3.9 The profiles of a droplet water on the surface of polyimide film (a) fluorine-containing polyimide (b) non-fluorine-containing polyimide.	30
Figure 3.10 Structure of polyimide (1) fluorine-containing polyimide (2) non-fluorine-containing polyimide. Structure of dianhydride (a) 6FDA (b) BTDA. Structure of polyimide derived from 6FDA (1a and 2a) and structure of polyimide derived from BTDA (1b and 2b).	31
Figure 3.11 Transmission UV-visible absorption spectra of fluorine-containing polyimide film and non-fluorine-containing polyimide film.	32
Figure 4.1 Model reaction of PBA-a/6FDA.	39
Figure 4.2 Model reaction of PBA-4fa/6FDA.	40
Figure 4.3 Model reaction of PBAF-a/6FDA.	41
Figure 4.4 Model reaction of PBAF-4fa/6FDA.	42
Figure 5.1 The structures of fluorine-containing benzoxazine monomers: (a) BA-4fa, (b) BAF-a and (c) BAF-4fa and traditional benzoxazine: (d) BA-a.	44
Figure 5.2 Appearance of benzoxazine monomers (a) BA-4fa, (b) BAF-a, (c) BAF-4fa and (d) BA-a.	44
Figure 5.3 FTIR spectra of benzoxazine monomers: (a) BA-a, (b) BAF-a, (c) BA-4fa and (d) BAF-4fa.	60

- Figure 5.4** FTIR spectra of fluorine-containing benzoxazine monomer (a) BAF-a and fluorine-containing polybenzoxazine (b) PBAF-a.61
- Figure 5.5** FTIR spectra of (a) PBA-a, (b) 6FDA, (c) PBAF-a/6FDA 1/1, (d) PBAF-a/6FDA 2.5/1 and (e) PBAF-a/6FDA 5/1.62
- Figure 5.6** The appearance color of PBAF-a/6FDA at various ratios (a) PBAF-a/6FDA 1/1, (b) PBAF-a/6FDA 2/1, (c) PBAF-a/6FDA 2.5/1, (d) PBAF-a/6FDA 3/1, (e) PBAF-a/6FDA 4/1 and (f) PBAF-a/6FDA 5/1.63
- Figure 5.7** DSC thermograms of fluorine-containing benzoxazine blending with 6FDA at 2.5/1 mole ratio at various conditions: (●) 80°C 1 h, (■) 130°C 1 h, (◆) 150°C /1 h, (▲) 170°C /1 h, (▲) 210°C /1 h and (▼) 240°C /2 h.64
- Figure 5.8** DSC thermograms of PBAF-a/6FDA at various mole ratios: (●) PBAF-a/6FDA 1/1, (■) PBAF-a/6FDA 2/1, (◆) PBAF-a/6FDA 2.5/1, (▲) PBAF-a/6FDA 3/1, (▼) PBAF-a/6FDA 4/1, (▲) PBAF-a/6FDA 5/1 and (▲) PBAF-a.65
- Figure 5.9** Storage modulus of PBAF-a/6FDA at various mole ratios: (●) PBAF-a/6FDA 1/1, (■) PBAF-a/6FDA 2/1, (◆) PBAF-a/6FDA 2.5/1, (▲) PBAF-a/6FDA 3/1, (▼) PBAF-a/6FDA 4/1, (▲) PBAF-a/6FDA 5/1, (▲) PBAF-a and (○) PBA-a.66
- Figure 5.10** Loss modulus of PBAF-a/6FDA at various mole ratios: (●) PBAF-a/6FDA 1/1, (■) PBAF-a/6FDA 2/1, (◆) PBAF-a/6FDA 2.5/1, (▲) PBAF-a/6FDA 3/1, (▼) PBAF-a/6FDA 4/1, (▲) PBAF-a/6FDA 5/1, (▲) PBAF-a and (○) PBA-a.67
- Figure 5.11** Thermal degradation PBAF-a/6FDA at various mole ratios: (●) PBAF-a/6FDA 1/1, (■) PBAF-a/6FDA 2/1, (◆) PBAF-a/6FDA 2.5/1, (▲) PBAF-a/6FDA 3/1, (▼) PBAF-a/6FDA 4/1, (▲) PBAF-a/6FDA 5/1, (▲) PBAF-a and (○) PBA-a.68
- Figure 5.12** Thermal degradation temperature at 10% weight loss and char yield of PBAF-a/6FDA at various 6FDA content.69
- Figure 5.13** Rate of weight loss PBAF-a/6FDA at various mole ratios: (●) PBAF-a/6FDA 1/1, (■) PBAF-a/6FDA 2/1, (◆) PBAF-a/6FDA 2.5/1, (▲) PBAF-a/6FDA 3/1, (▼) PBAF-a/6FDA 4/1, (▲) PBAF-a/6FDA 5/1, (▲) PBAF-a, (○) PBA-a and (□) 6FDA.70

Figure 5.14 TMA curves of PBAF-a/6FDA at various mole ratios: (●) PBAF-a/6FDA 1/1, (■) PBAF-a/6FDA 2/1, (◆) PBAF-a/6FDA 2.5/1, (▲) PBAF-a/6FDA 3/1, (▼) PBAF-a/6FDA 4/1, (▴) PBAF-a/6FDA 5/1 and (▲) PBAF-a.....71

Figure 5.15 Photographs of PBAF-a/6FDA at various ratios: (a) PBAF-a/6FDA 1/1, (b) PBAF-a/6FDA 2/1, (c) PBAF-a/6FDA 2.5/1, (d) PBAF-a/6FDA 3/1, (e) PBAF-a/6FDA 4/1 and (f) PBAF-a/6FDA 5/1.....72

Figure 5.16 The optimum radius of curvature of PBAF-a/6FDA at various ratios: (a) PBAF-a/6FDA 1/1, (b) PBAF-a/6FDA 2/1, (c) PBAF-a/6FDA 2.5/1, (d) PBAF-a/6FDA 3/1, (e) PBAF-a/6FDA 4/1 and (f) PBAF-a/6FDA 5/1.....73

Figure 5.17 Appearance of water contact angle of PBAF-a/6FDA at various mole ratios: (a) PBAF-a/6FDA 1/1, (b) PBAF-a/6FDA 2/1, (c) PBAF-a/6FDA 2.5/1, (d) PBAF-a/6FDA 3/1, (e) PBAF-a/6FDA 4/1, (f) PBAF-a/6FDA 5/1, (g) PBAF-a and (h) PBA-a.74

Figure 5.18 Water contact angle of PBAF-a/6FDA at various 6FDA content.....75

CHAPTER I

INTRODUCTION

1.1 Overview

Fluorine is well known chemical as the most electronegative element in the periodical table as displayed in Figure 1.1. The fluorine atoms generally have high thermal and chemical stability [1]. The low polarity of fluorine gives a low refractive index, low surface free energy, as well as low dielectric constant which make it highly attractive raw material to be used for electronics applications [2]. Fluorine-containing polymers are a class of high - performance polymeric materials containing fluorine atoms in the polymer structure. Consequently, these polymers exhibit some outstanding characteristics inherited from this atom such as chemical resistance, thermal stability, low surface energy, flame resistance and low dielectric constant [3, 4] A large variety of high performance fluorine - containing polymers including epoxy resins [5, 6], polyimides [7], cyanate esters [8] and polybenzoxazines [9, 10] These polymers have been synthesized and characterized to be used for commercial applications. Lists trade names, companies, properties and applications of some important fluorine-containing polymers currently available in the market.

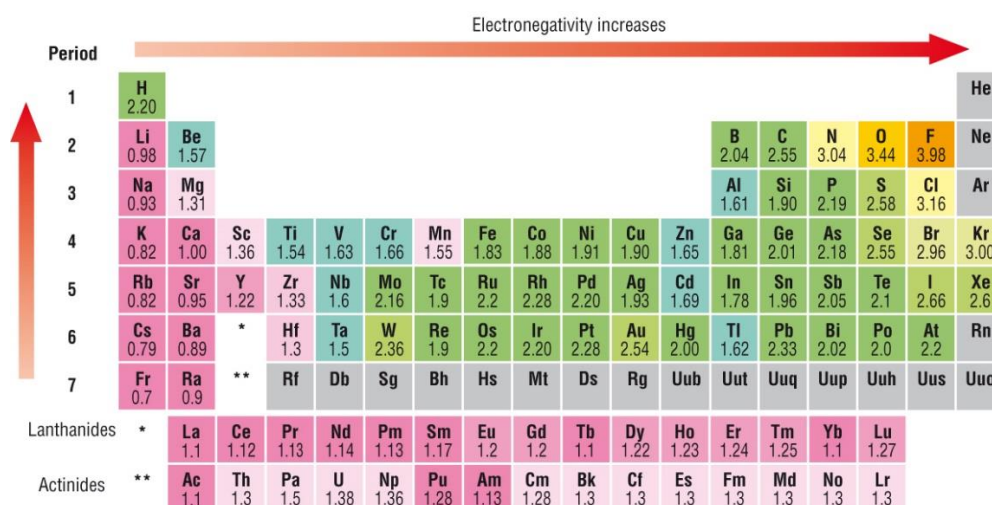


Figure 1.1 Electronegativity of the elements in the periodic table suggesting fluorine atom into possess the highest value [11].

Table 1.1 Summary of trade names, companies, applications and properties of major fluorine-containing polymers

Companies	Products	Properties	Applications
Changshu Zhongzun Space Flight Insulating Material Co., Ltd	(Polyimide Fluorine 46) Composite Film (HTFEP)	<ul style="list-style-type: none"> • Electric insulating • Resistance to height temperature • Radiation and corrosion under high temperature 	<ul style="list-style-type: none"> • Microelectronic applications
NeXolve Corporation	CORIN XLS Polyimide	<ul style="list-style-type: none"> • Optically transparent 	<ul style="list-style-type: none"> • Display applications

		<ul style="list-style-type: none"> • high glass transition temperature greater than 250°C 	
NeXolve Corporation	CP1 Polyimide	<ul style="list-style-type: none"> • Highly transparent • Low dielectric constant • Low moisture uptake • UV resistant 	<ul style="list-style-type: none"> • Display applications • Space structures • Thermal insulation • Electrical insulators • Industrial tapes • Advanced composites
Q-Mantic	HF/FHF Polyimide-Fluorine-46 Composite Film (F06)	<ul style="list-style-type: none"> • Electric insulating • Resistance to high temperature • Radiation and corrosion under high temperature 	<ul style="list-style-type: none"> • Layers of wire cable • Electromagnetic
Daikin America	OPTODYNE UV (fluorine-containing epoxy)	<ul style="list-style-type: none"> • Constant refractive index 	<ul style="list-style-type: none"> • Reliable adhesive

Recent development of a new class of phenolic resins such as polybenzoxazines have yield new materials. These raw material have attractive characteristics with outstanding properties such as good thermal stability, good mechanical properties, high glass transition temperature (T_g), high char yield, low flammability, low water absorption and low dielectric constant [12]. Furthermore, polymerization of benzoxazine resins proceeds through ring - opening mechanism of the cyclic monomers only by heat treatment without catalyst and without harmful by - product during the cure process [13]. However polybenzoxazines have some inherent shortcomings i.e. their brittleness after curing, thus limits certain applications. This problem can be overcome relatively easily as these types of resins can be conveniently modified [14].

To further improve the performance of polybenzoxazine, there are two main approaches [15, 16]. The first approach is the modification of the structure of benzoxazine monomers with an introduction of other functional units or other molecular moieties. This could be one effective method to enhance properties of the resulting polybenzoxazine. For example, the modification of benzoxazine structures using bisphenol-S [17], bisphenol-AP [18], bisphenol-AF [10] have been reported. Chang et al. [10] synthesized fluorinated benzoxazine resin (BAF-4fa) by using bisphenol-AF, 4-(trifluoromethyl)aniline and paraformaldehyde as reagents. It was observed that thermal properties such as glass transition temperature (T_g), degradation temperature (T_d) and char yield of BAF-4fa polybenzoxazine was significantly higher than those of

bisphenol-A-aniline based polybenzoxazine (PBA-a). Moreover, they also investigated properties of the copolybenzoxazine of BAF-4fa type and BA-a type. The obtained copolybenzoxazine at 50/50 wt% showed a relatively low dielectric constant of 2.36 comparing with the value of about 3.56 of the polybenzoxazine without fluorine atom in its structure.

The second approach is the alloy formation of polybenzoxazine with other monomers, resins or polymers to enhance its properties such as the alloys of polybenzoxazine with polyurethanes [16, 19], epoxy [20], polyimide [16] and anhydride [21, 22]. Jubsilp et al. [23] reported properties of bisphenol-A-aniline based polybenzoxazine (PBA-a) enhanced by alloying with various types of anhydrides. The alloy films were prepared from mixtures of BA-a resin with three different aromatic carboxylic dianhydrides i.e. pyromellitic dianhydride (PMDA), 3,3',4,4' bizophenonetetracarboxylic dianhydride (BTDA) and 3,3',4,4' biphenyltetracarboxylic dianhydride (s-BPDA). The authors reported that the copolymer films showed excellent thermal stability with very high glass transition temperature. The T_g value of neat PBA-a was reported to be 178°C while the T_g values of the resulting copolymers i.e., PBA-a : PMDA, PBA-a : BTDA and PBA-a : s-BPDA were found to be 300°C, 263°C and 270°C, respectively. Moreover, degradation temperature (T_d) at 10% weight loss of the alloy films was determined in the range of 410 - 426°C and the highest char yield at 800°C was found to be approximately 60%, which was more than twice greater than that of the neat PBA-a. In addition, the copolymer films exhibited excellent toughness

due to the formation of additional ester linkages obtained PBA-a by copolymer networks.

As dianhydride is one of the monomer used in polyimide synthesis. Effects of fluorine-containing dianhydride on properties of the resulting polyimide have also been investigated. There are also several researches that used fluorine-containing dianhydrides i.e. 4,4'-(hexafluoroisopropylidene)diphthalic anhydride (6FDA) to synthesize polyimide. Jang et al. [24] reported that polyimides synthesized by fluorinated dianhydride and diamines. With the incorporating of strong electron withdrawing CF_3 groups in the dianhydride moiety in their synthesis, the color of the polyimide can be changed to a lighter one as reported the yellow index (YI) value. The YI value of polyimide based on fluorine-containing 6FDA monomer was also found to be approximately 18% lower than that of polyimide based on BTDA. In general, highly transparent and almost colorless film specimens with low dielectric constant have been obtained in 6FDA containing polyimides [25-28].

The objective of this study will be to modify benzoxazine resins employing two approaches. In the first approach modification process will be carried out by using fluorine-containing biphenol and fluorine-containing primary amine while alloy formation using fluorinated benzoxazine monomers with fluorine-containing dianhydride will be the second approach. The essential properties of the resulting fluorine-containing polybenzoxazine alloys such as their thermal, mechanical and physical properties will be evaluated.

1.2 Objectives

- 1.2.1 To synthesize fluorine-containing benzoxazine i.e. BA-4fa, BAF-a and BAF-4fa using solventless synthesis.
- 1.2.2 To study suitable mole ratio of polymeric systems between fluorine-containing benzoxazine modified with 4,4'-(hexafluoroisopropylidene)diphthalic anhydride (6FDA) on its curing and processing conditions.
- 1.2.3 To evaluate thermal, mechanical and physical properties of fluorine-containing polybenzoxazine modified with 4,4'-(hexafluoroisopropylidene)diphthalic anhydride (6FDA).

1.3 Scopes of research

- 1.3.1 Synthesis fluorine-containing benzoxazine based on bisphenol-A, and 4-trifluoromethyl aniline (BA-4fa), bisphenol-AF and aniline (BAF-a), bisphenol-AF, and 4-trifluoromethyl aniline (BAF-4fa). These material using solventless synthesis.
- 1.3.2 Preparation of polymeric systems between the fluorine-containing benzoxazine modified with 4,4'-(hexafluoroisopropylidene)diphthalic anhydride (6FDA) at various mole ratios i.e. 5:1, 4:1, 3:1, 2:1, and 1:1.

1.3.3 Examination of thermal mechanical and physical properties of the polymeric alloys using

- Fourier Transform Infrared Spectroscopy (FTIR : Functional group)
- Differential Scanning Calorimeter (DSC : curing condition)
- Thermogravimetric analyzer (TGA : T_d , Char yield)
- Dynamic Mechanical Analyzer (DMA : T_g , modulus)
- Contact Angle Analyzer (Contact Angle, Surface free energy)
- Dielectric Analyzer (Dielectric constant)
- Solvent Extraction (Ability of network formation)
- Thermal Mechanical Analyzer (TMA : T_g , CTE)
- Flexibility (Radius of curvature)

CHAPTER II

THEORY

2.1 Benzoxazine resin

Polybenzoxazines are a newly developed class of thermosetting resins that have been developed as a novel type of phenolic resin. Benzoxazine monomers are easily prepared from phenol, formaldehyde and amine by using solventless synthesis technology [29]., which can be classified into monofunctional and bifunctional types depending on a type of phenol used as shown in Figure 2.1 and Figure 2.2, respectively.

Polybenzoxazine are obtained by thermally induced ring-opening polymerization of benzoxazines monomer taking place without catalyst or curing agents required, without harmful by-products during cure and low melt viscosity. Polybenzoxazine shows outstanding properties such as excellent electrical, thermal and mechanical properties, near-zero volumetric shrinkage upon polymerization and low water absorption.

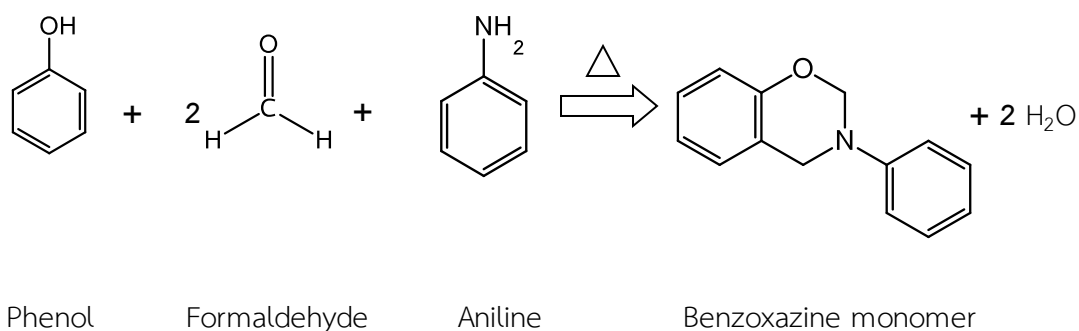


Figure 2.1 Schematic synthesis of monofunctional benzoxazine monomer.

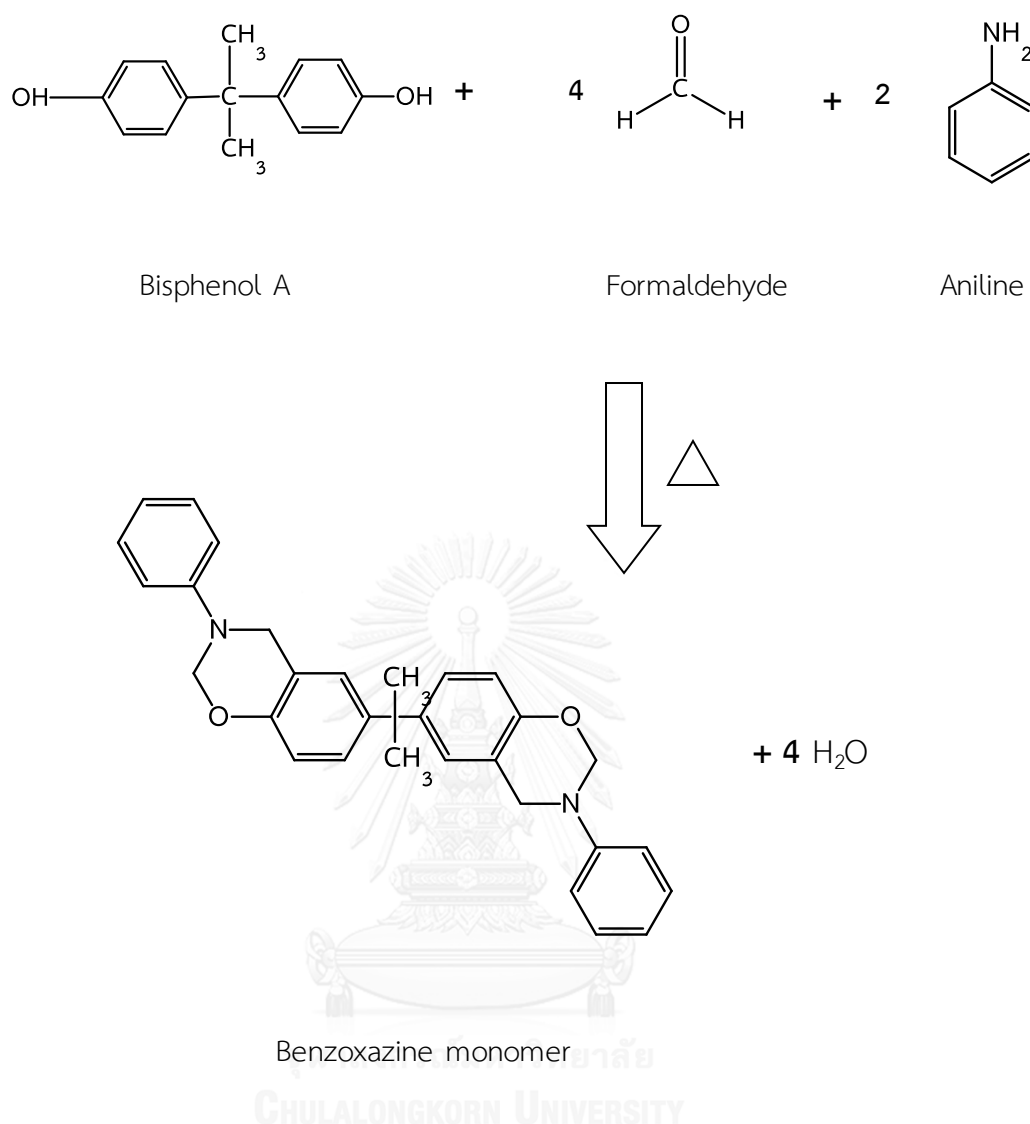


Figure 2.2 Schematic synthesis of bifunctional benzoxazine monomer.

2.2 Fluorine – containing polymers

Fluorine – containing polymers are the polymeric materials containing fluorine atoms in their chemical structures. The properties of fluorine – containing polymers such as chemical resistance, thermal stability, low coefficient of friction, low surface energy, and low dielectric constant are reported. Moreover, they have weather stability, high volume and surface resistivity and flame resistance [3].

Due to their special chemical and physical properties, the fluoropolymers are widely applied in the chemical, electrical/electronic, construction, architectural, and automotive industries as displayed in Table 2.1 [30].

The incorporation of fluorine atom into polymers structure is able to achieve materials with high thermal stability and low dielectric constant. Fluorination can improve thermal properties of the samples because the C-F bond is stronger than the C-H [31]. They can reduce the dielectric constant due to its lower polarizability structure as well as the increase in free volume which result in low intermolecular energy and efficient low chain packing [32].

Table 2.1 Applications of fluoropolymers

Industry/ Application Area	Key Properties
Chemical Processing	Chemical resistance, mechanical properties, thermal stability, weather stability
Electrical and Communications	Dielectric constant, flame resistance, thermal stability, high volume/surface resistivity, high dielectric breakdown voltage

Automotive and Office Equipment	Low coefficient of friction , good mechanical properties, thermal properties , chemical resistance, cryogenic properties, friction property
Houseware	Thermal stability, low surface energy, chemical resistance
Medical	Low surface energy, biological stability, excellent mechanical properties, chemical resistance
Architectural Fabric	Excellent weatherability, flame resistance Low surface energy, friction property, thermal stability
Semiconductor Fabrication	Chemical resistance, purity, non-shedding, thermal stability

2.3 Bisphenol-A

Bisphenol-A or 4,4'-Isopropylidenediphenol is a colorless crystalline solid belonging to the family of organic compounds, its molecular formula is $C_{15}H_{16}O_2$. It is soluble in organic solvents, but poorly soluble in water [33].

Bisphenol-A is an industrial chemical that is widely used in the production of polycarbonate (PC) plastics to manufacture food contact materials, such as baby bottles and food containers and epoxy resins, protective linings for canned foods and beverages and as a coating on metal lids for glass jars and bottles [34, 35].

Moreover, Bisphenol-A is the main ingredient used for production of unsaturated polyester and polysulfone resins [36].

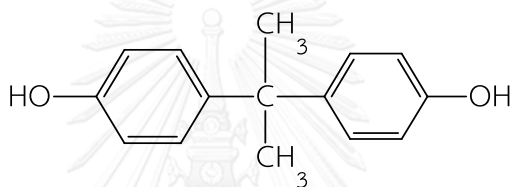


Figure 2.3 Bisphenol-A used in benzoxazine synthesis.

Table 2.2 Physical and chemical properties of bisphenol-A [37]

Synonym	4,4'-Isopropylidenediphenol 2,2-Bis(4-hydroxyphenyl)propane,
Appearance / Colour	Cystalline / Beige
Melting Point	158 - 159°C
Boiling Pont	220 °C at 5 hPa - lit.
Molecular Formula	C ₁₅ H ₁₆ O ₂
Molecular Weight	228.29 g/mol

2.4 Bisphenol-AF

Bisphenol-AF has been successfully used as a monomer in the synthesis of other specialty polymers, including polyimides, polyamides, polyesters, and polycarbonates. Such polymers are used in various a wide range of specialty applications, e.g. in gas separation and semiconductor processing [38].



Figure 2.4 Bisphenol-AF used in benzoxazine synthesis.

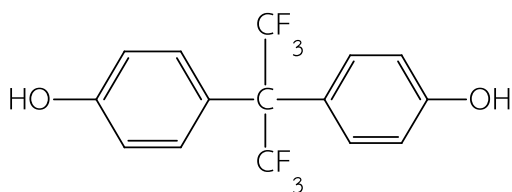


Figure 2.5 Structure of bisphenol-AF.

Table 2.3 Physical and chemical properties of bisphenol-AF [39, 40]

Synonym	4,4'-(Hexafluoroisopropylidene)diphenol 2,2-Bis(4-hydroxyphenyl)hexafluoropropane Hexafluorobisphenol A
Appearance / Colour	Powder / Beige
Melting Point	160 - 163°C
Boiling Point	400°C
Molecular Formula	C ₁₅ H ₁₀ F ₆ O ₂
Molecular Weight	336.23 g/mol

2.5 Formaldehyde

The formaldehyde has been widely used to decontaminate laboratory tools and facilities. It is also most commonly used raw material as an adhesive in wood composite panel production [41, 42]. The formula of formaldehyde is CH₂O and it is a white crystalline powder with a light pungent odor [41, 43]. When it is heated, formaldehyde gas is emitted, which is the actual decontaminant. It is known that formaldehyde is hazardous chemical to human and environment. It is also flammable so that certain precautions need to be considered for any applications [43].



Figure 2.6 Paraformaldehyde powder used in benzoxazine synthesis.

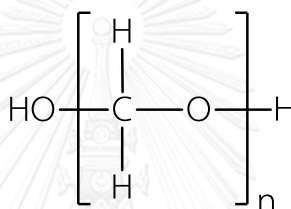


Figure 2.7 Structure of paraformaldehyde.

Table 2.4 Physical and chemical properties of paraformaldehyde [44]

Appearance	Powder
Ignition Temperature	300°C
Melting Point	100 - 130°C
Molecular Formula	(CH ₂ O) _n
Molecular Weight	30.03 g/mol
Density	1.4 g/cm ³ at 20°C
Solubility	Slightly soluble at 20°C

2.6 Aniline

Aniline is the commonly material to use in manufacturing. Aniline is primarily used in MDI foams for the automotive and construction industries. Many chemicals can be made from aniline, including: Isocyanates for the urethane industry, Indigo, acetoacetanilide and other dyes and pigments for a variety of applications. Diphenylamine for the rubber, petroleum, plastics, agricultural, explosives. Chemical industries. Pharmaceutical, organic chemical, and other products [45].



Figure 2.8 Aniline used in benzoxazine synthesis.

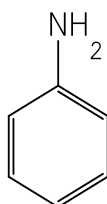


Figure 2.9 Structure of aniline.

Table 2.5 Physical and chemical properties of aniline [44]

Appearance	Liquid/ Colorless
Melting Point	-6°C
Boiling Point	184°C
Molecular Formula	C ₆ H ₅ NH ₂
Molecular Weight	93.13 g/mol

2.7 4-(trifluoromethyl)aniline

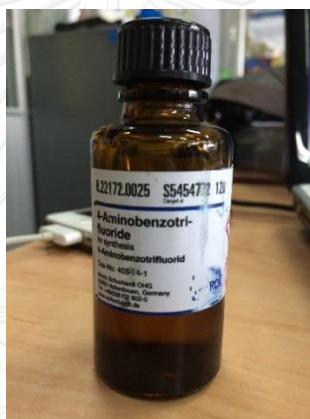


Figure 2.10 4-(trifluoromethyl)aniline used in benzoxazine synthesis.

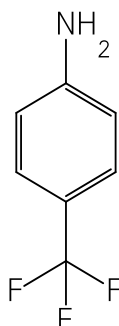


Figure 2.11 Structure of 4-(trifluoromethyl)aniline.

Table 2.6 Physical and chemical properties of 4-(trifluoromethyl)aniline [46].

Appearance	liquid
Melting Point	3 - 8°C
Boiling Point	82 - 84°C (16 hPa)
Molecular Formula	C ₇ H ₆ F ₃ N
Molecular Weight	161.12 g/mol

2.8 Anhydride

4,4'-(hexafluoroisopropylidene)diphthalic anhydride, widely known as 6FDA or 6F-dianhydride is a monomer for specialty polyimides. Typically, high performance polyimides containing 6FDA are used in application areas where thermal stability, low thermal expansion properties, low dielectric constants, or precise control of optical transparency and refractive indices are required. They are desirable raw materials in manufacture of membranes, aerospace, or microelectronics applications [41].

**Figure 2.12** 4,4'-(hexafluoroisopropylidene)diphthalic anhydride (6FDA).

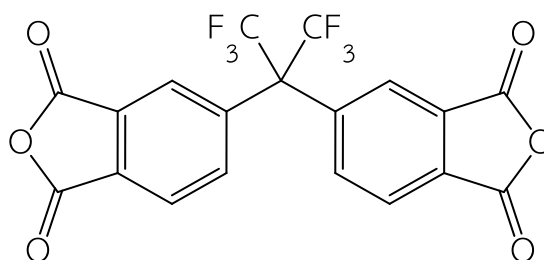


Figure 2.13 Structure of 4,4'-(hexafluoroisopropylidene)diphthalic anhydride (6FDA).

Table 2.7 Physical and chemical properties of 4,4'-(hexafluoroisopropylidene)diphthalic anhydride (6FDA) [43, 47]

Appearance / Colour	Powder crystalline /White
Melting Point	244 -247°C
Boiling Pont	494.5°C at 760 mmHg
Flash Point	243.7°C
Molecular Formula	C ₁₉ H ₆ F ₆ O ₆
Molecular Weight	444.24 g/mol

2.9 N,N-Dimethylacetamide

N,N-dimethylacetamide is an excellent solvent with high solvating power for high molecular weight polymers and synthetic resins. DMAc is used as a reaction solvent for the manufacture of acryl and polyamide fibers. DMAc is also used for the manufacture of agro chemicals, dyes and pharmaceuticals [48].

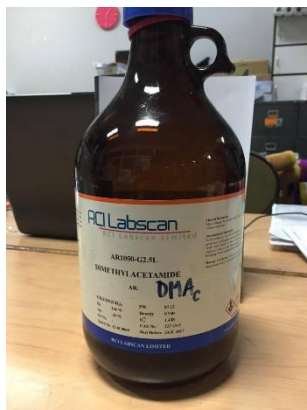


Figure 2.14 N,N-dimethylacetamide.

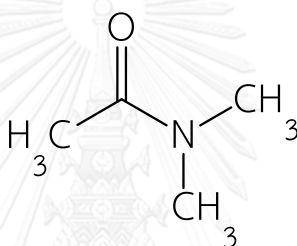


Figure 2.15 Structure of n,n-dimethylacetamide (DMAc).

Table 2.8 Physical and chemical properties of n,n-dimethylacetamide (DMAc) [49]

Appearance / Colour	Liquid / Colorless to yellow
Melting Point	- 20°C
Boiling Point	166°C
Flash Point	70°C
Molecular Formula	CH ₃ CON(CH ₃) ₂
Molecular Weight	87.12 g/mol

CHAPTER III

LITERATURE REVIEWS

Y. C. Su, and F. C. Chang (2003) [10] prepared polybenzoxazine with low dielectric constant for use as insulating material. In their study, a novel structure of the fluorinated benzoxazine (BAF-4fa) was synthesized by incorporating the trifluoromethyl groups into the monomer as illustrated in Figure 3.1. Furthermore, they prepared the fluorinated copolybenzoxazine with different ratios of bisphenol-A-aniline-based benzoxazine (BA-a) and as synthesized benzoxazine BAF-4fa type. The obtained copolybenzoxazine was depicted in Figure 3.2. The results showed that the incorporation of fluorinated substitution decreased the dielectric constant of the copolybenzoxazine. The value of the neat BA-a decreased from 3.56 to 2.36 of those with one mole ratio of BAF-4fa benzoxazine in the copolybenzoxazine as showed in Table 3.1. The copolymers with low dielectric constant are suitable for insulating applications. With an increase in BAF-4fa benzoxazine content in the copolybenzoxazine, glass transition temperature and degradation temperature increased as well.

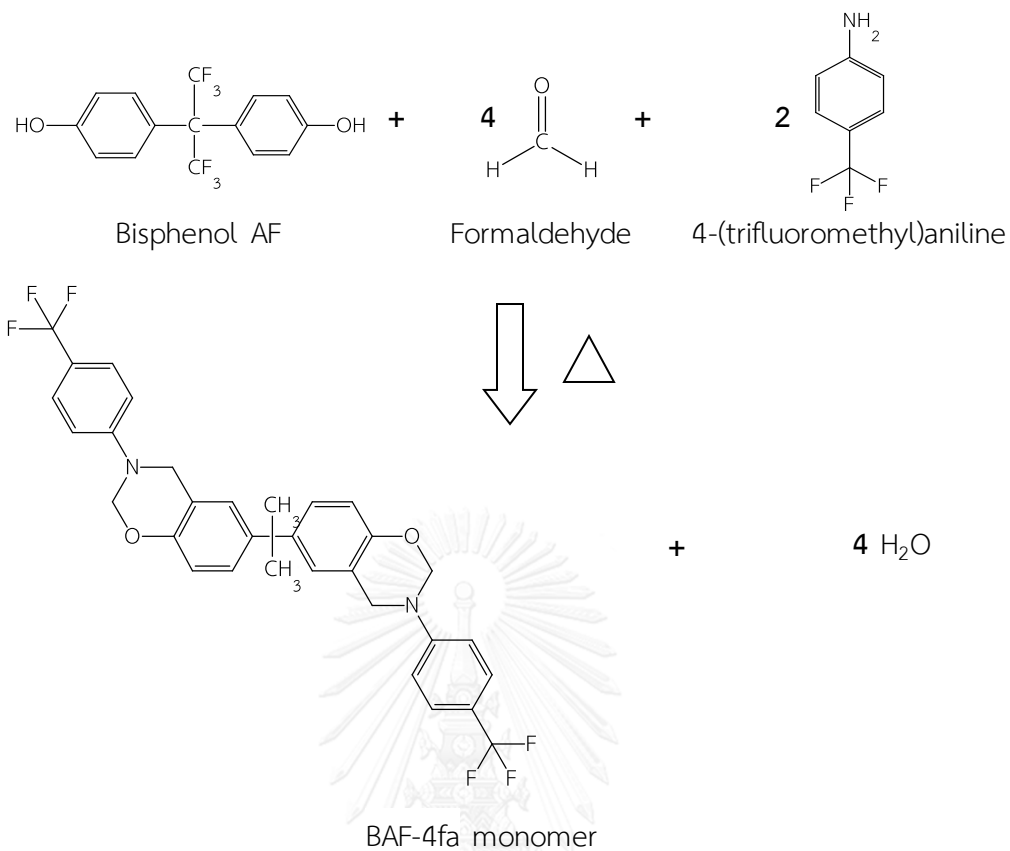


Figure 3.1 Schematic synthesis of fluorine-containing benzoxazine monomer.

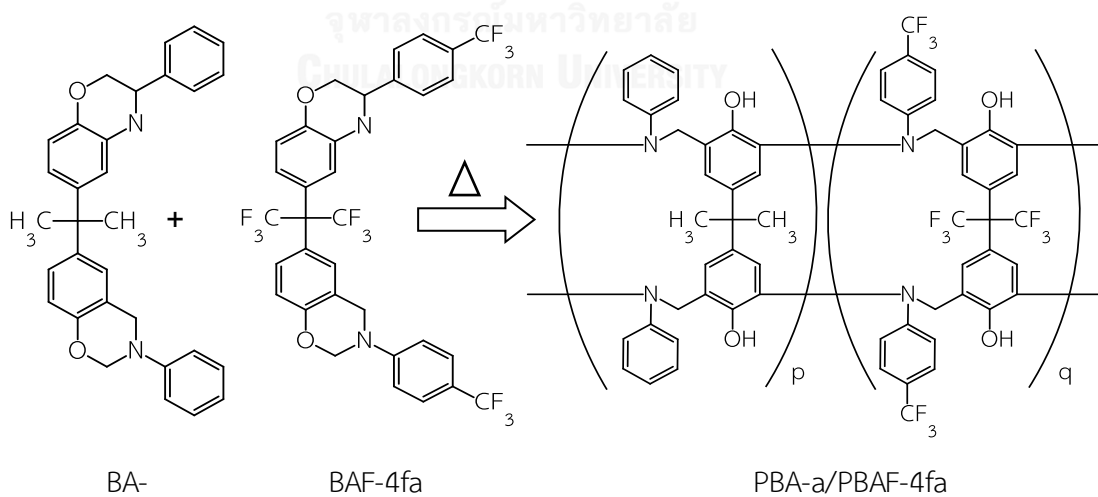


Figure 3.2 The structure of copolybenzoxazine with PBA-a/PBAF-4fa.

Table 3.1 Properties of copolybenzoxazine

BA-a / BAF-4fa (weight ratio)	Properties		
	Dielectric constant	T _g (°C)	Td ₁₀ (°C)
1/0	3.56	170.6	363.6
1/0.05	3.02	176.6	366.1
1/0.1	2.85	186.3	379.7
1/0.2	2.76	197.0	400.2
1/0.5	2.39	235.8	420.6
1/1	2.36	264.9	430.6
0/1	-	283.4	455.7

The FTIR spectra of BAF-4fa monomer was observed in this research as shown in Figure 3.3. The characteristic absorption band of oxazine ring was found at 937 cm⁻¹ whereas the band at 1521 cm⁻¹ was attributed to the tri-substituted benzene ring and CH₂ wagging. was appeared at 1242 cm⁻¹, Moreover the band at 1238 cm⁻¹ was found C-F stretching.

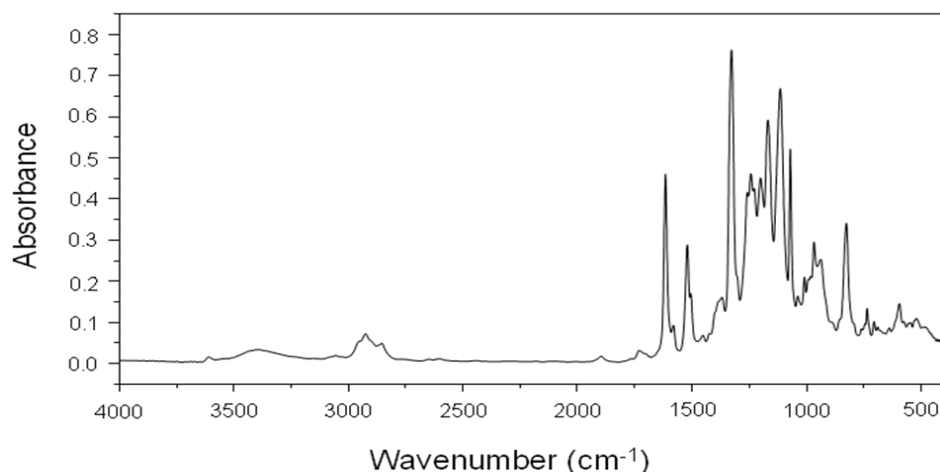


Figure 3.3 FTIR spectra of BAF-4fa monomer.

C. Jubsilp, et. al. (2012) [23] reported properties enhancement of bisphenol-A-aniline based polybenzoxazine (PBA-a) by alloying with three different aromatic carboxylic dianhydrides i.e. pyromellitic dianhydride (PMDA), 3,3',4,4' bizophenonetetracarboxylic dianhydride (BTDA) and 3,3',4,4' biphenyltetracarboxylic dianhydride (s-BPDA). The reaction model of alloy films was shown in Figure 3.4. From FTIR spectra, the carbonyl stretching bands of aromatic dianhydrides at 1780 cm^{-1} and 1860 cm^{-1} were disappeared whereas an ester linkage was observed at 1730 cm^{-1} , indicating the reaction between phenolic hydroxyl groups of PBA-a and anhydride groups of aromatic dianhydrides as can be seen in Figure 3.5

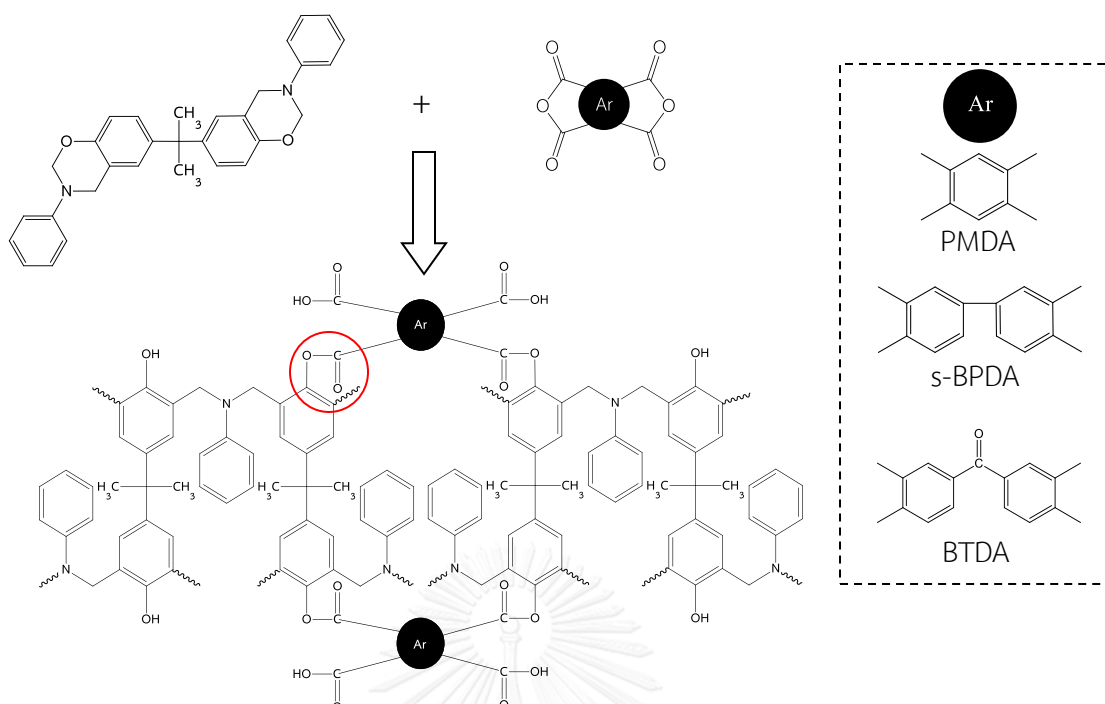


Figure 3.4 Structure of the alloy films.

The formation of the ester linkage was found to help improve flexibility of the alloy films compared to the neat PBA-a film as shown in Figure 3.6 (a) and Figure 3.6 (b). Furthermore, the T_g and T_d of the alloy films with the incorporation of aromatic anhydrides were higher than those of the neat PBA-a film. The alloy film of BA-a and PMDA possessed the highest thermal properties. Crosslink density of PBA-a was greatly enhanced by an addition of PMDA, s-BPDA or BTDA, corresponding to an enhancement in their T_g values. The values were also summarized in Table 3.2

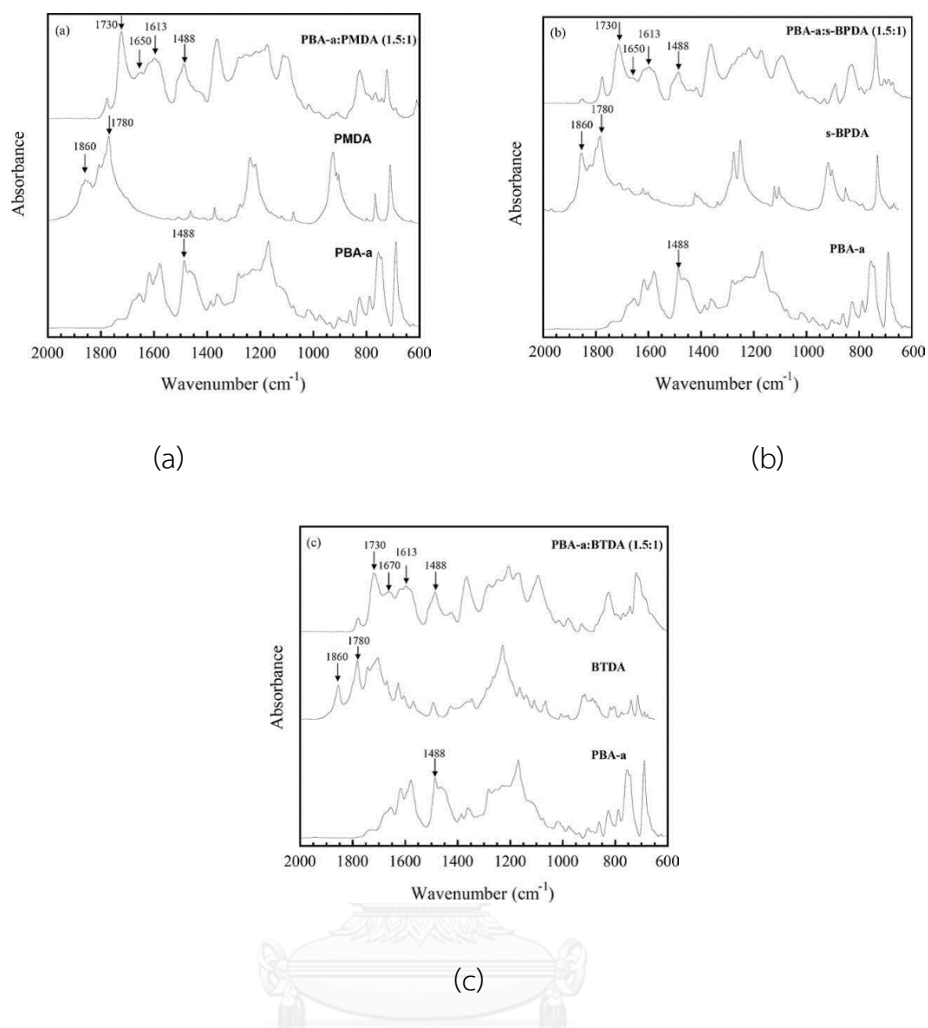


Figure 3.5 FTIR spectra of PBA-a alloy with aromatic dianhydrides: (a) PBA-a: PMDA, (b) PBA-a : s-BPDA and (c) PBA-a : BTDA.

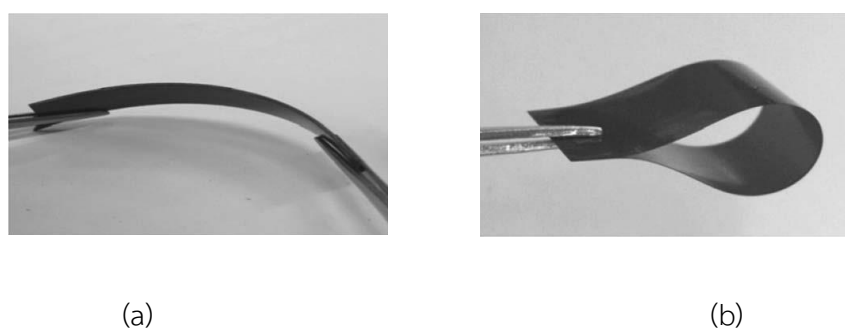


Figure 3.6 Appearance of alloy films: (a) PBA-a, (b) PBA-a alloy with aromatic dianhydrides.

Table 3.2 Properties of PBA-a and PBA-alloys with aromatic dianhydrides

Sample (mole ratio)	Properties		
	T _g (°C)	Td ₁₀ (°C)	Crosslink density (mol/cm ³)
PBA-a	178	361	3981
PBA-a : PMDA (1.5 : 1)	300	426	8656
PBA-a : s-BPDA (1.5 : 1)	263	422	7664
PBA-a : BTDA (1.5 : 1)	270	410	7630

W., Jang et al. (2007) [24] synthesized polyimides films with difference of dianhydrides i.e. 3,3',4,4'-Benzophenonetetracarboxylic dianhydride (BTDA), 4,4'-oxydiphthalic anhydride (ODPA) and 4,4'-(Hexafluoroisopropylidene)diphthalic anhydride (6FDA). The color intensity of the obtained polyimides were explained from lightness (L*), yellowness (b*) and redness (a*). The most films polyimides were accurate experiment to measure yellowness on yellow index (YI) values. Figure 3.7 showed that the YI of polyimides were affected by diamine moieties, which decreased in order of series 6 > 4 > 5 of polyimides films. The series 6a polyimide film showed the highest value of YI whereas 5c polyimide film with four CF₃ groups in the polyimide exhibited the lightest color.

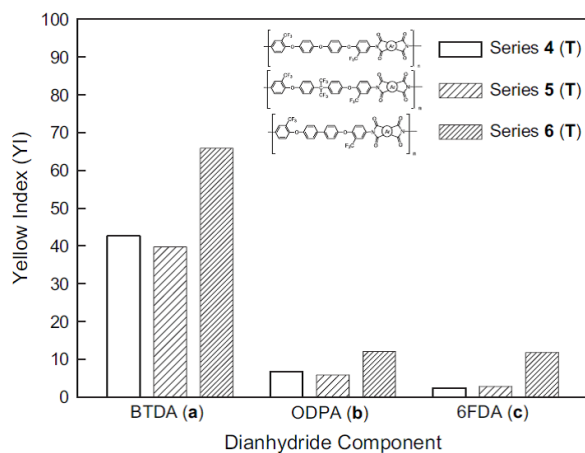


Figure 3.7 Yellow index value of polyimides films.

C., Wang et al. [50] synthesized fluorine-containing polyimide film (a) and non-fluorine-containing polyimide film (b) as shown in Figure 3.8. The values of contact angle and surface free energy of the two polyimides were investigated. As seen in Table 3.3, fluorine-containing polyimide film showed higher contact angle than non-fluorine-containing polyimide as illustrated in Figure 3.9. In contrast, surface free energy which decreased with an incorporation of fluorine in polyimide structure. The results indicated that fluorine-containing polyimide film showed relatively hydrophobic behavior.

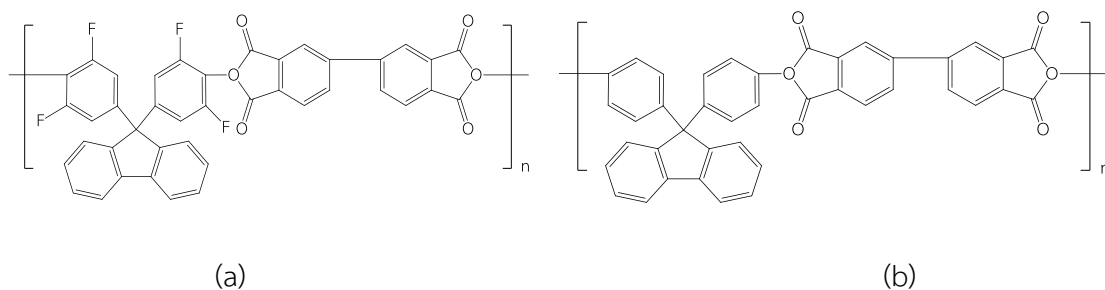


Figure 3.8 Structure of polyimides (a) fluorine-containing polyimide and (b) non-fluorine-containing polyimide.

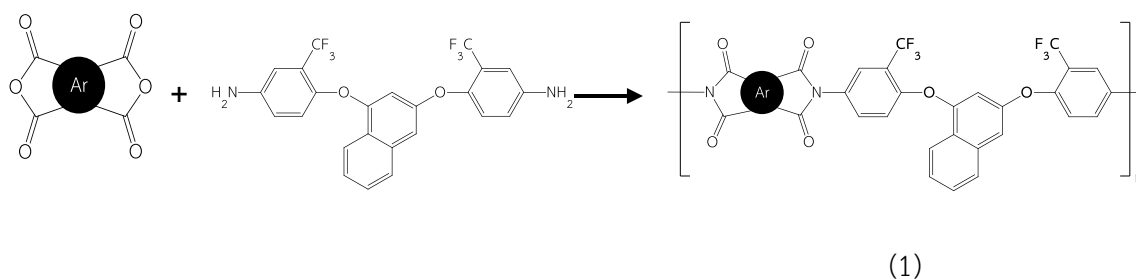
Table 3.3 Contact angle and surface free energy of polyimide films

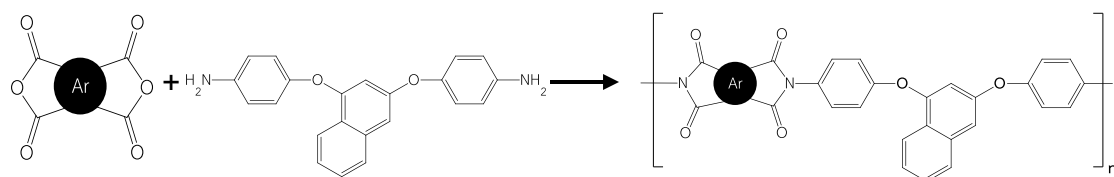
Polyimide	Contact angle (°)	Surface energy (mJ/m ²)
Fluorine-containing polyimide	107.9	16.39
Non-fluorine-containing polyimide	91.4	24.46



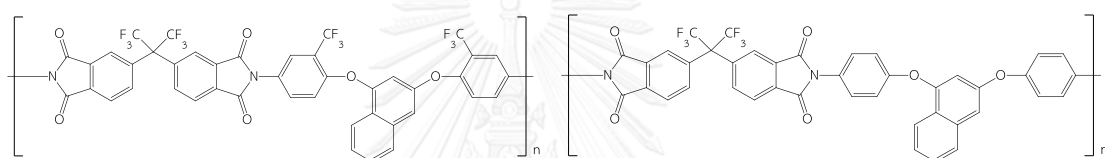
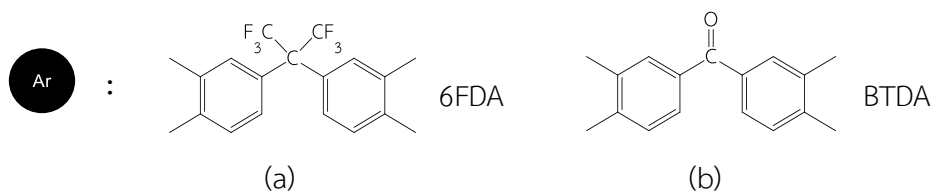
Figure 3.9 The profiles of a droplet water on the surface of polyimide film (a) fluorine-containing polyimide and (b) non-fluorine-containing polyimide.

S. H., Hsiao et al. [51] were synthesized polyimide from diamine [1,3-bis(4-amino-2-trifluoromethylphenoxy)] and dianhydrides (BTDA and 6FDA etc.) showed in Figure 3.10



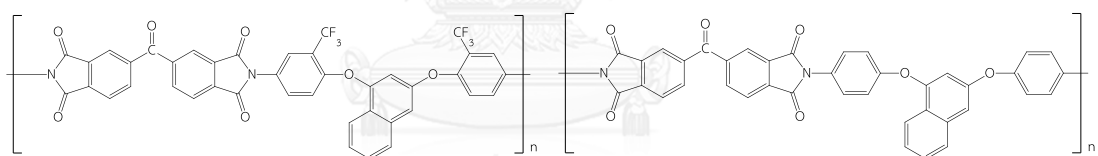


(2)



(1a)

(2a)



(1b)

(2b)

Figure 3.10 Structure of polyimide (1) fluorine-containing polyimide, (2) non-fluorine-containing polyimide. Structure of dianhydride (a) 6FDA, (b) BTDA. Structure of polyimide derived from 6FDA (1a and 2a) and structure of polyimide derived from BTDA (1b and 2b).

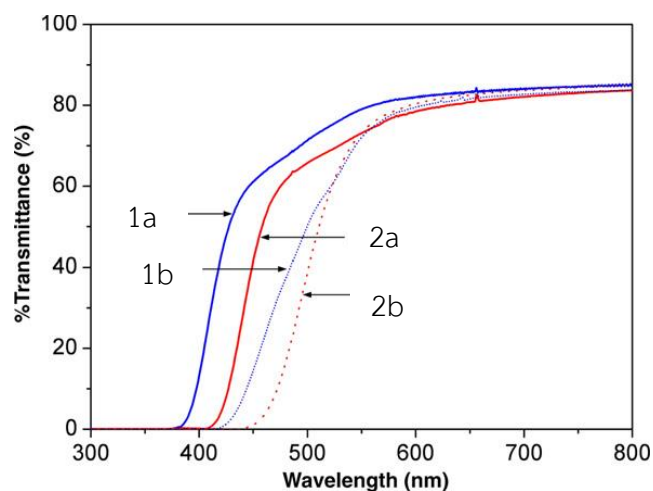


Figure 3.11 Transmission UV-visible absorption spectra of fluorine-containing polyimide film and non-fluorine-containing polyimide film.

The color intensities of polyimide films were explained from redness (a^*), yellowness (b^*) and lightness (L^*). As seen in Table 3.4, yellowness values of the fluorine-containing polyimides films was lower than non-fluorine-containing polyimides films. Furthermore, transparency of polyimide films was also measured by using UV visible spectroscopy. Figure 3.11 showed the transmittance UV-vis spectra of polyimide films and cutoff wavelength (λ_0) from UV-vis spectra was shown in Table 3.4. As the results, fluorine-containing polyimide films revealed lower λ_0 than those of CF_3 -free structure. The 6FDA dianhydride provided transparent and colorless polyimide films in contrast to the other dianhydride. The bulky and electron-withdrawing CF_3 groups in diamine was effective in reduced CTC formation between polymer chains through steric hindrance and the inductive effect. The positive effect of CF_3 groups in polyimide films is the weakened intermolecular force due to lower polarizability of C-F bond.

Table 3.4 Color coordinates and cutoff wavelength λ_0 from UV-vis spectra of the polyimide films.

Polymer	Redness (a*)	Yellowness (b*)	Lightness (L*)	Cutoff wavelength : λ_0 (nm)
1a	-4.1	13.4	94.3	383
2a	-5.0	40.4	84.9	402
1b	-6.8	35.6	85.1	414
2b	-29.2	87.6	65.5	468

CHAPTER IV

EXPERIMENTAL

4.1 Raw materials

Chemical and solvents used in this research are bisphenol-AF or 4,4'-(hexafluoroisopropylidene)diphenol (97%) and 6FDA or 4,4'-(Hexafluoroisopropylidene)diphthalic anhydride were obtained from Sigma-Aldrich Co., Ltd. Paraformaldehyde (AR grade) and 4-(trifluoromethyl)aniline were purchased from Merck Ltd. Aniline (AR grade) (99%) was purchased from Panreac Quimica S.A. N-N'-dimethylacetamide (DMAC) as a solvent was obtained from RCL labscan Co., Ltd. All chemicals were used as received.

4.2 Synthesis of fluorine-containing benzoxazine monomer

Benzoxazine monomers are typically synthesized using phenol, formaldehyde and aniline as starting materials are based on solventless synthesis technology [29]. Various types of benzoxazine monomer can be synthesized using various phenol derivatives and amines with different substitution groups attached. In this work, fluorine-containing benzoxazine monomers have been synthesized with three types of monomers. First, BA-4fa was synthesized from bisphenol-A, paraformaldehyde and 4-(trifluoromethyl)aniline. Second, BAF-a was synthesized from bisphenol-AF, paraformaldehyde and aniline. Third, BAF-4fa was synthesized from bisphenol-AF, paraformaldehyde and 4-(trifluoromethyl)aniline. All of fluorine-containing

benzoxazine monomers were synthesized by solventless technology at a molar ratio of phenol derivatives, formaldehyde and amines were 1: 4: 2 respectively. The reactants were heated at 110°C in an aluminum pan and continuously stirred for 15-20 minutes to yield a light yellow solid benzoxazine monomer which was ground into fine powder.

4.3 Preparation of the 6FDA based polybenzoxazine alloy films

6FDA based polybenzoxazine alloy films i.e. PBA-a/6FDA, PBAF-a/6FDA, PBA-4fa/6FDA and PBAF-4fa/6FDA were proposed reaction models in Figure 4.1- Figure 4.4

6FDA based polybenzoxazine alloy films were prepared by blending benzoxazine based 6FDA alloy films at various mole ratios (benzoxazine/6FDA) i.e. 1/1, 1.5/1, 2/1, 2.5/1, 3/1, 4/1 and 5/1. The 6FDA based polybenzoxazine alloy films were dissolved in DMAc and then the mixtures were continuously stirred for 15 - 20 minutes with magnetic stirrer at 90°C until clear homogenous mixtures were obtained. The clear homogenous mixtures solution of 6FDA based polybenzoxazine alloy films were cast on glass plates and thickness of alloy films were about 100 μm . Then the partly solvent was evaporated at room temperature overnight. The samples were heated in an air-circulated oven at 60°C, 80°C, 110°C, 130°C for each 1 h. and then, the samples were cured at 150°C, 170°C, 190°C, 210°C, 230°C for 1 h each and 240°C for 2 hours temperature to guarantee complete cure of the samples. After completion of the curing, the samples were allowed to free cool down to room temperature overnight.

4.4 Characterizations of the 6FDA based polybenzoxazine alloy films

4.4.1 Fourier transform infrared spectroscopy (FTIR)

Chemical structure of fluorine-containing benzoxazine monomers and network formation of BAF-a and 6FDA based polybenzoxazine alloy films were determined using Fourier transform infrared (FTIR) spectroscopy, a Spectrum GX FTIR spectrometer from Perkin Elmer. Transmission spectra were obtained by casting a thin film of the mixtures solution on a potassium bromide (KBr) plate or silicon wafer. All spectra were taken as a function of time with 128 scans at a resolution of 4 cm^{-1} and in a spectra range of $4000\text{-}400\text{ cm}^{-1}$.

4.4.2 Differential scanning calorimetry (DSC)

Differential scanning calorimetry (DSC1, Mettler-Toledo International Inc, Switzerland) was performed to study curing behaviors of samples. The mass of the sample is in the range of 3 - 5 mg for monomer sample and 8 - 10 mg for polymer sample which were take samples in aluminum pans with lids. All experiments were conducted at a heating rate of $10^{\circ}\text{C}/\text{min}$ from 30°C to 350°C under a constant nitrogen atmosphere at a flow rate of $50\text{ ml}/\text{min}$.

4.4.3 Dynamic mechanical analysis (DMA)

Dynamic mechanical analysis (DMA) (DMA, model DMA24, NETZSCH, Germany) was used to investigated dynamic mechanical properties and relaxation behaviors of the obtained polybenzoxazine and 6FDA based polybenzoxazine alloy

films. The test was performed in the tensile geometry at 1 Hz with a strain value of 0.1% and at a heating rate of 2°C/min from 30°C to 420°C under nitrogen purging rate of 80 mL/min. The dimension of the specimen was 5 mm × 10 mm × 0.10 mm. (W×L×H)

4.4.4 Thermogravimetric analysis (TGA)

Thermogravimetric analysis to study thermal stability of the samples was performed on TGA1 STAR_e system from Mettler - Toledo International Inc. The testing temperature program was ramped at a heating rate of 20°C/min from 30°C to 850°C under nitrogen atmosphere with a constant flow rate of 50 mL/min. The sample mass used was measured to be approximately 10 mg. The degradation temperature (T_d) and char yield of the samples were reported at their 10% weight loss and at 800°C, respectively.

4.4.5 Thermal mechanical analysis (TMA)

Thermal mechanical analysis was performed with a Mettler Toledo Instruments TMA/SDTA1 at heating rate 10°C/min from 30°C to 320°C under nitrogen atmosphere and under force of 20 mN. The coefficient of thermal expansion (CTE) was measured in the range 30°C to 150°C.

4.4.6 Dielectric constant

The dielectric constant was performed on LCR meter which determine the dielectric constant of 6FDA based polybenzoxazine alloy films at 100 kHz. The

dielectric constant of each alloy film was an average of the dielectric constant from five specimens.

4.4.7 Radius of curvature (Flexibility of alloy films)

The flexibility of 6FDA based polybenzoxazine alloy films can be test by bending the alloy films at the various positions. The dimension of the alloy films was 1 cm × 5 cm × 0.01 cm. The different scale of each position alloy films is 0.2 cm. Bending test the films using the forceps clamp at the position of 0.2 cm to 2 cm and recorded the diameter of the alloy films

4.4.8 Water contact angle

The water contact angle droplets about 10 μL on the alloy films was measured using a contact angle meter from Tantec Inc. Model 2500702 and capture the images of the water droplets on the surface of alloy films at room temperature (25°C). The water contact angle of each alloy film was an average of the water contact angles from five times at different locations on each film.

4.4.9 Solvent extraction

The solvent extraction of 6FDA based polybenzoxazine alloy films measured after completely cured at 240°C. The specimen is 2.0 cm × 2.0 cm × 0.01 cm. The alloy films were immersed in 10 ml of chloroform as the solvent to determine the nature of crosslinking network formation. The mass of the residual solid was weighed in every 7 days for 30 days immersion.

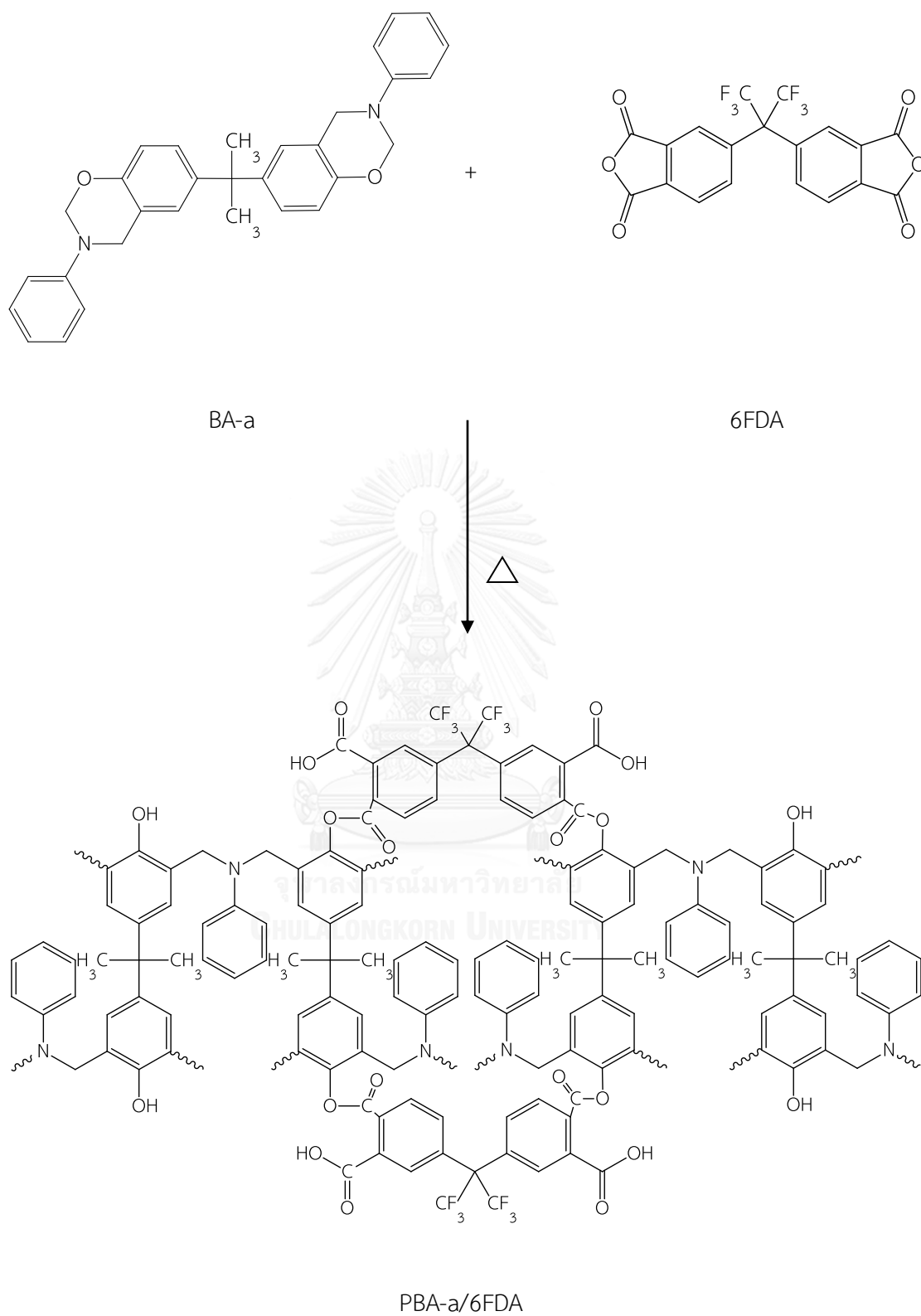


Figure 4.1 Model reaction of PBA-a/6FDA.

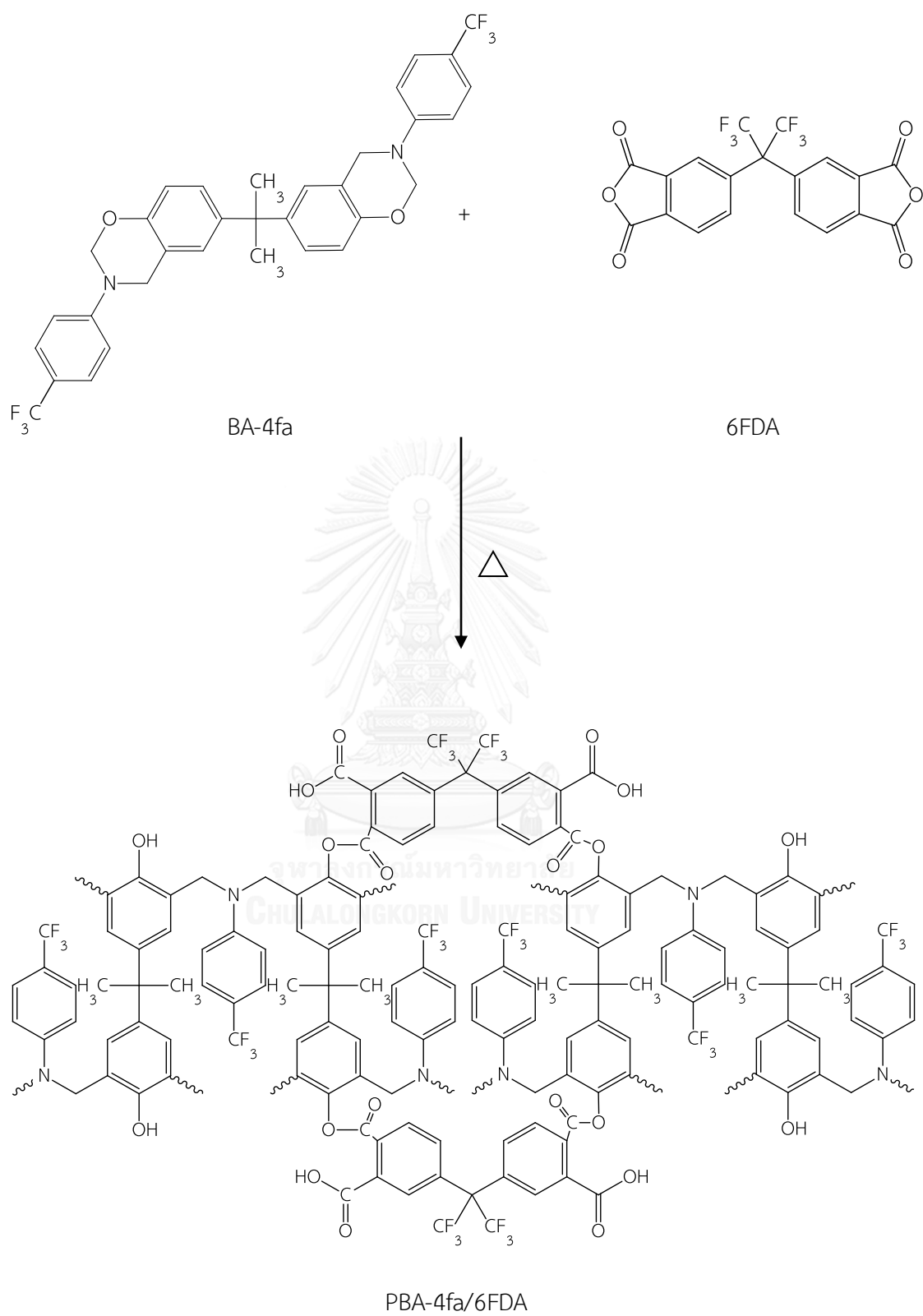


Figure 4.2 Model reaction of PBA-4fa/6FDA.

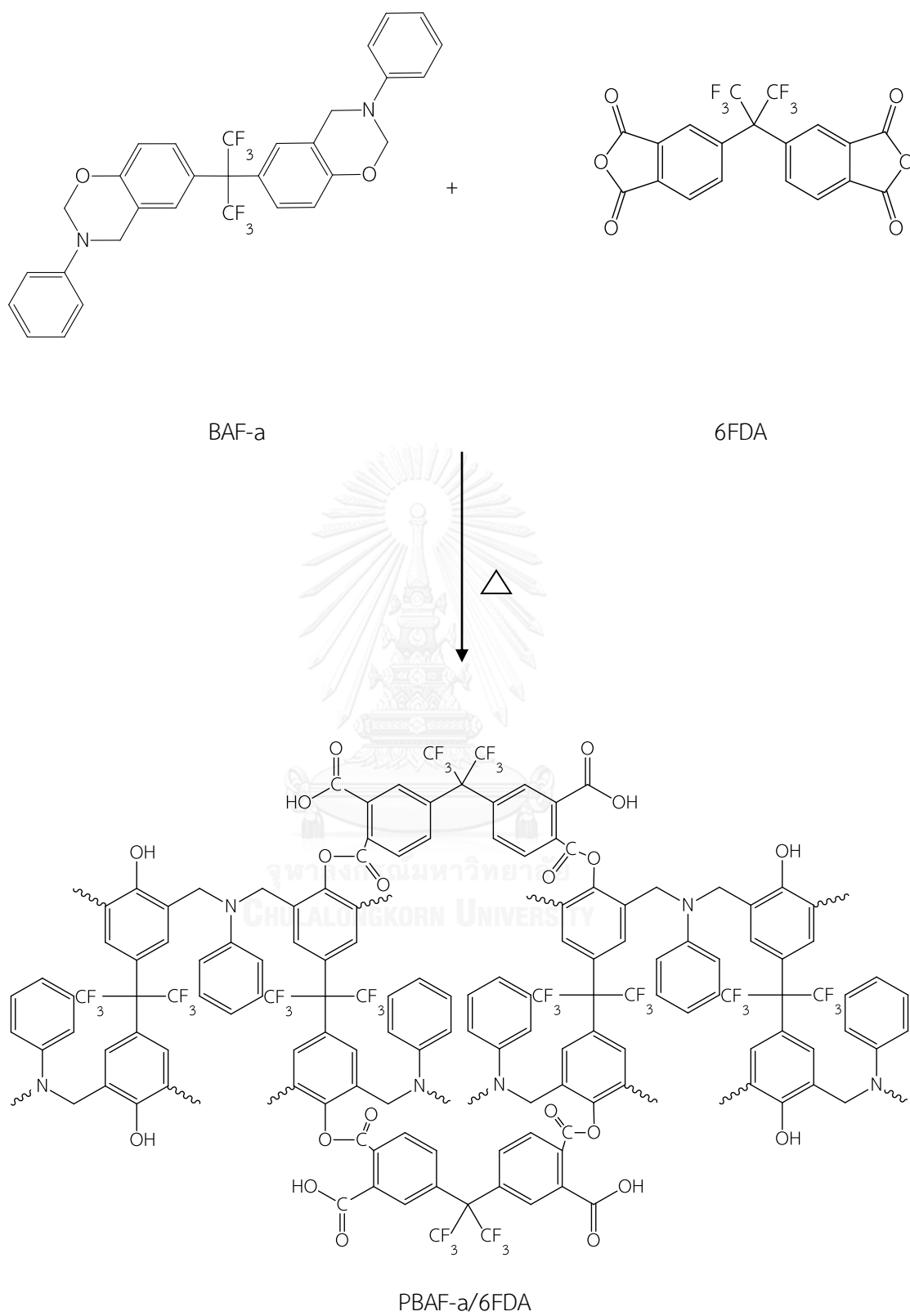


Figure 4.3 Model reaction of PBAF-a/6FDA.

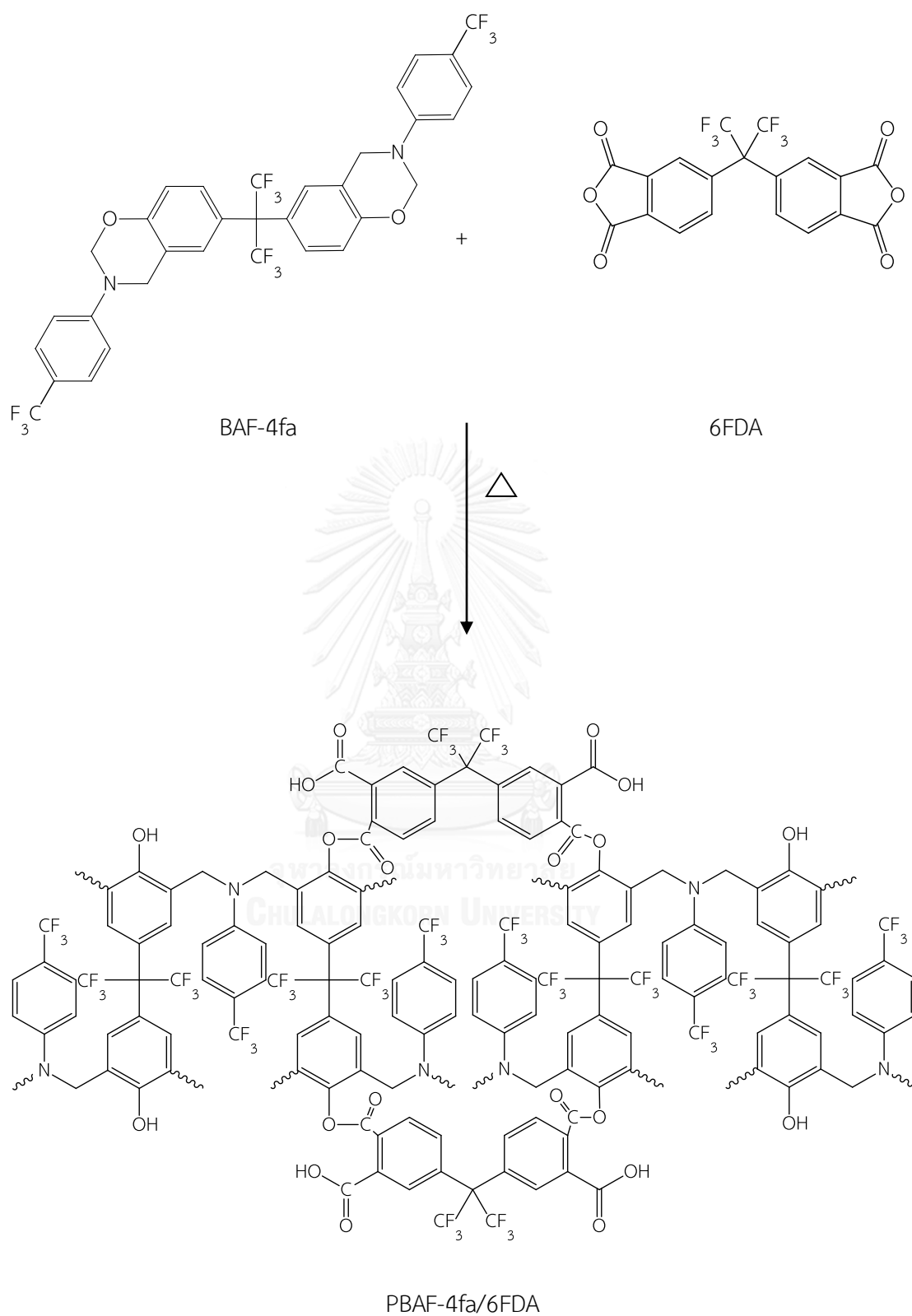


Figure 4.4 Model reaction of PBAF-4fa/6FDA.

CHAPTER V

RESULTS AND DISCUSSION

5.1 Preparation and characterization of fluorine-containing benzoxazine monomers

5.1.1 Preparation of fluorine-containing benzoxazine monomers.

Three types of fluorine-containing benzoxazine monomers i.e. BA-4fa, BAF-a and BAF-4fa which can be successfully synthesized by solventless technology and the chemical structures of the obtained resins compared with traditional benzoxazine monomer (BA-a) are displayed in Figure 5.1. These monomers have been synthesized using phenol derivatives, paraformaldehyde and primary amine at a mole ratio of 1 : 4 : 2 respectively and synthesized using the same condition i.e. at 110°C for 15 - 20 minutes. The monomers were then cooled down at room temperature and ground into fine powder. Figure 5.2 shows yellow and light yellow solid of fluorine-containing benzoxazine resins and traditional benzoxazine (BA-a)

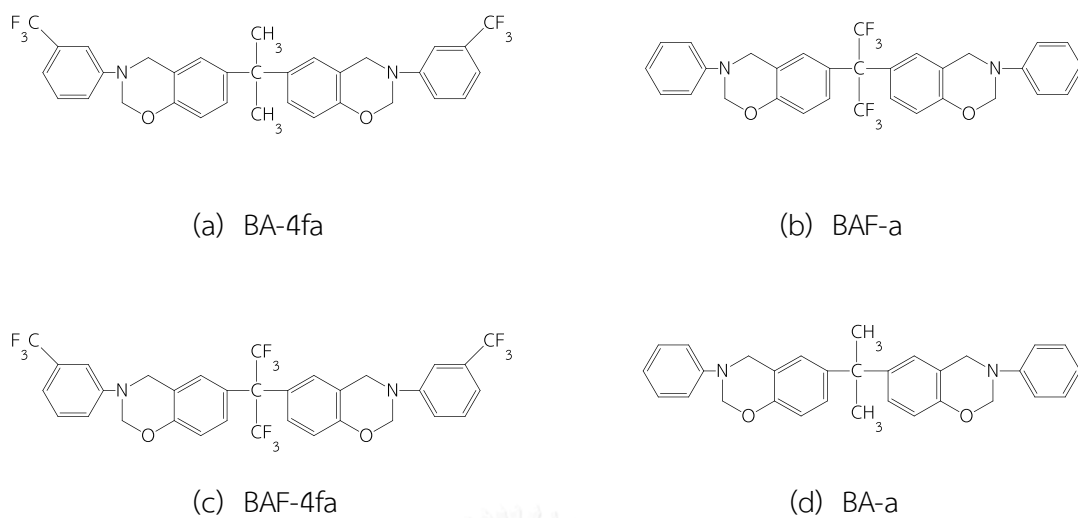


Figure 5.1 The structures of fluorine-containing benzoxazine monomers: (a) BA-4fa, (b) BAF-a and (c) BAF-4fa and traditional benzoxazine: (d) BA-a.

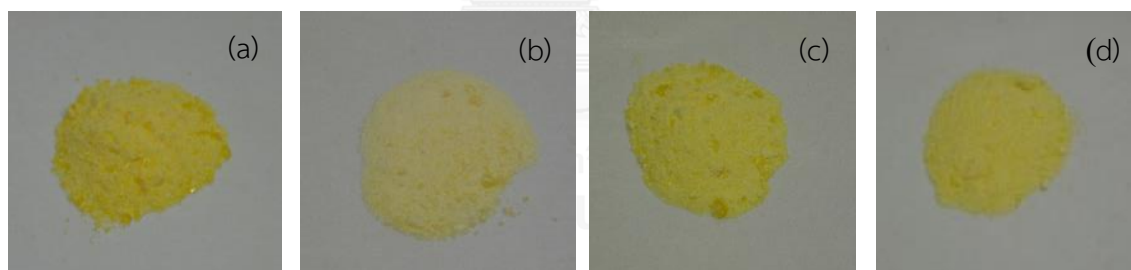


Figure 5.2 Appearance of benzoxazine monomers (a) BA-4fa, (b) BAF-a, (c) BAF-4fa and (d) BA-a.

5.1.2 Characterizations of fluorine-containing benzoxazine monomers by fourier transform infrared (FTIR) spectroscopy and thermogravimetric analyzer (TGA)

The chemical structures of fluorine-containing benzoxazine monomers i.e. BA-4fa, BAF-a and BAF-4fa compared with traditional benzoxazine monomer (BA-a) have been confirmed by FTIR spectra as shown in Figure 5.3. All chemical structures of BAF-4fa, BAF-a, BAF-4fa and BA-a were found to possess the same oxazine ring characteristics. For example, infrared absorption bands that were attributed to the tri-substituted benzene ring attached to the oxazine ring are observed in the range of 1505 - 1499 cm^{-1} . Asymmetric and symmetric stretching aromatic ether (C-O-C) group of oxazine ring was found in a range of 1244 - 1231 cm^{-1} and 1069 - 1029 cm^{-1} respectively whereas the band in a range of 1168 - 1151 cm^{-1} was attributed to asymmetric stretching of a C-N-C group. The bands at 693 and 755 - 753 cm^{-1} were assigned to the benzene ring with five adjacent free hydrogen atoms [52]. Moreover, the fluorine-containing benzoxazine monomers were found to reveal the characteristic peaks of fluorine structure i.e. C-F stretching was found at 1260 - 1112 cm^{-1} and CF_3 attached to the aromatic ring were found in BA-4fa and BAF-4fa to be a range of 1329 - 1328 cm^{-1} . Normally, the structures of the pure benzoxazine monomers do not contain phenolic hydroxyl group (-OH) but in Figure 5.3 showed the broad peak around 3400 cm^{-1} which suggests the presence of some ring opened structures of the benzoxazine oligomers in these resins.

In addition, TGA data showed the degradation temperature at 5% and 10% weight loss of BAF-4fa synthesized by solventless method ($Td_5 = 379^\circ\text{C}$ and $Td_{10} = 453^\circ\text{C}$) compared with those of BAF-4fa synthesized by a traditional solvent method as reported by Su Y.-C. et al. [10] ($Td_5 = 374^\circ\text{C}$ and $Td_{10} = 456^\circ\text{C}$). It can be seen that the solventless synthesis used in this work provides exactly the same BAF-4fa monomer or this monomer is successfully prepared by a solventless synthesis which is a more environmentally friendly and a more cost effective technique.

5.2 Preparation and characterization of 6FDA modified polybenzoxazine alloy films

5.2.1 Preparation of 6FDA modified polybenzoxazines alloy films

6FDA modified polybenzoxazine alloy films i.e. PBA-4fa/6FDA, PBAF-a/6FDA, PBAF-4fa/6FDA and PBA-a/6FDA were prepared by blending benzoxazine monomer with 6FDA at various mole ratios (i.e. 1/1, 1.5/1, 2/1, 2.5/1, 3/1, 4/1 and 5/1) in dimethylacetamide (DMAc) solvent using total solid of 1.5 g in DMAc of 1.5 ml for all blending ratios. The mixtures were stirred at 90°C for 20 - 25 minutes until the mixtures became clear and transparent homogenous mixtures and were then cooled down to room temperature. The homogenous mixtures of 6FDA modified benzoxazine alloy of all ratios above are transparent light yellow to red in color. After that the homogeneous mixtures were cast on glass plate and kept at room temperature

overnight to settle the films and to partially remove the solvent. Then the solvent was further gradually removed at 60°C, 80°C, 110°C 130°C for 1 hour each, respectively. The films were cured in an air-circulated oven at 150°C, 170°C, 190°C, 210°C and 230 °C for 1 hour each, respectively and 240°C for 2 hours. All samples were allowed to free cool slowly overnight. The thickness of the resulting films were about 100 μm and the visual appearance of PBAF-a/6FDA alloy films is showed in Figure 5.6. It can be seen that, the yellow color of the PBAF-a/6FDA alloy films became lighter with an increase of the 6FDA content.

5.2.2 Characterization of 6FDA modified polybenzoxazines alloy films by using thermogravimetric analyzer (TGA)

From Table 5.1 reports T_{d_5} , $T_{d_{10}}$ and char yield at 800°C from the TGA of those fluorine-containing benzoxazine resins modified with 6FDA dianhydride to be compared with the previously reported non-fluorine containing systems [23, 53]. From the results, the values of $T_{d_{10}}$ at 2.5/1 mole ratio were found to be as follows: PBAF-a/6FDA (464°C) > PBA-4fa/6FDA (418°C) > PBAF-4fa/6FDA (417°C) > PBA-a/6FDA (387°C). Moreover, char yield at 2.5/1 mole ratio was found to be: PBAF-a/6FDA (56.0%) > PBA-4fa/6FDA (53.4%) > PBA-a/6FDA (53.0%) > PBAF-4fa/6FDA (47.7%). It can be seen that the $T_{d_{10}}$ value of PBAF-a/6FDA showed the highest value suggesting the presence of fluorine moiety in the main chain of the polymer (from bisphenol-AF) is crucial in enhancing thermal stability of the polymer. However, the replacement of aniline side

group with 4-(trifluoromethyl)aniline tends to provide lower thermal degradation temperature in the obtained benzoxazine resin suggesting the position of fluorine moiety in the benzoxazine network is also essential in improving its thermal stability. It is likely the fluorine moiety that is attached to the weak points in the polymer network such as aniline or 4-(trifluoromethyl)aniline on the Mannich bridge in our case, might be released first during the thermal decomposition. 4-(trifluoromethyl)aniline is greater in mass compared to aniline thus the observed lower T_{d10} value of PBAF-4fa/6FDA compared to PBAF-a/6FDA above. Additional factors of choosing appropriate materials for engineering applications are their cost and processability. The reactants to synthesize fully fluorinated BAF-4fa benzoxazine resin are more expensive than BAF-a benzoxazine resin. Moreover, it was also observed that PBA-4fa/6FDA and PBAF-4fa/6FDA allot films tend to crack into small pieces during the film casting process on glass substrate. Thus, these two alloy films cannot be further characterized based on the current film casting technique. For these reasons, BAF-a/6FDA alloy films are the suitable candidate for further property characterizations.

5.3 Fourier transform infrared spectroscopy (FTIR) study of 6FDA modified PBAF-a alloy films

The chemical structures of BAF-a, PBAF-a, 6FDA and PBAF-a/6FDA alloy films at 5/1, 2.5/1 and 1/1 mole ratio were confirmed by Fourier transform infrared (FTIR)

spectroscopy in Figure 5.4 (a) shows the important characteristics of infrared absorptions bands of BAF-a monomer to be centered at 966 and 1503 cm^{-1} , which is attributed to the tri-substituted benzene ring attached with oxazine ring while the bands at 1244 and 1029 cm^{-1} are assigned to asymmetric and symmetric stretching of aromatic ether C-O-C stretching group of oxazine ring, respectively. The band at 1151 cm^{-1} is attributed to asymmetric stretching of C-N-C group whereas the absorption band at 1198 cm^{-1} is assigned to the C-F stretching. Furthermore, the tri-substituted benzene ring at 966 and 1503 cm^{-1} in BAF-a monomer has been weakened with increased temperature. These characteristic infrared absorption bands completely disappeared, indicating the completion of ring-opening reaction of the oxazine ring after fully cured at 240°C. Meanwhile, the new absorption bands around at 1482 and 865 cm^{-1} as displayed in Figure 5.4 (b) which are assigned to tetra-substituted benzene ring, has led to the formation of Mannich bridge linkage and phenolic hydroxyl groups [18, 54]. Moreover, the ring-opening reaction of BAF-a monomer upon thermal treatment can also be observed through the appearance of a broad peak at 3400 cm^{-1} which is assigned to the phenolic hydroxyl group formation. This formation of hydroxyl group was expected to react with anhydride group of 6FDA material in the next alloying step.

For 6FDA material, the major vibrations band of the cyclic anhydride group assigned to the symmetric and asymmetric stretching of the carbonyl group (C=O) in

anhydride [52, 55] can be observed at 1861 and 1765 cm^{-1} respectively, as presented in Figure 5.5 (b)

The chemical formation of PBAF-a/6FDA alloy film at 5/1, 2.5/1 and 1/1 mole ratios is shown in Figure 5.5 (c) - (e). Moreover, the completely cured process being monitored in FTIR bands of carbonyl group of 6FDA in 1/1 mole ratio at 1861 and 1765 cm^{-1} were partly disappeared as shown in Figure 5.4 (c) and 5/1, 2.5/1 mole ratios were completely disappeared as seen in Figure 5.5 (d) - (e). It is implied that the mixing ratios of 2.5/1 and 5/1 provide the complete consumption of the anhydride whereas at 1/1 mole ratio of the mixture, the anhydride is an excess reactant and some of this chemical remains in the obtained alloy network. The reaction between the phenolic hydroxyl group of the PBAF-a and the dianhydride group of 6FDA was confirmed by the appearance of the band in the range of 1729 - 1724 cm^{-1} attributed to carbonyl stretching band of ester linkage [21-23, 53]. Additionally, open chain of anhydride after thermal curing process has resulted in the carboxylic acid in PBAF-a/6FDA alloy films which shows C=O stretching in the range of 1626 - 1623 cm^{-1} , C-O stretching and C-O-H in plane and out of plane bending at 1256-1255 cm^{-1} , 1440-1434 cm^{-1} and 965 cm^{-1} , respectively.

5.4 Differential scanning calorimetry (DSC) study of 6FDA modified PBAF-a alloy films

PBAF-a/6FDA alloy films were produced by blending fluorine-containing benzoxazine monomer with dianhydride in dimethylacetamide (DMA_c) at various mole ratio. Figure 5.7 illustrates the PBAF-a/6FDA alloy film at 2.5/1 mole ratio selected to be studied for the optimal curing condition by DSC using a heating rate of 10 °C/min under nitrogen atmosphere and in the temperature range of 30 - 320 °C. From DSC thermograms, after the films were kept at room temperature overnight, the PBAF-a/6FDA alloy film was dried at 80 °C and part of DMA_c solvent was removed by heat. The PBAF-a/6FDA alloy film showed the endothermic peak around 160 - 180 °C, which corresponded to the boiling point of DMA_c solvent (b.p. of DMA_c = 166 °C [49]). This endothermic peak decreased with an increasing temperature and completely disappeared after heat treatment at 170 °C. This indicated that the DMA_c as a solvent was completely removed from the PBAF-a/6FDA alloy film. Moreover, the area under exothermic peak at 240 °C decreased with an increasing temperature and completely disappeared after curing at 240 °C and showed glass transition temperature at about 260 °C.

Figure 5.8 provides the glass transition temperatures (T_g) of the neat PBAF-a and PBAF-a/6FDA alloy films at various mole ratios i.e. 1/1, 2/1, 2.5/1, 3/1, 4/1 and 5/1. From the DSC thermograms, the T_g is defined as the midpoint of the temperature range, bounded by the tangents to the two flat regions of the heat flow curve. T_g of

PBAF-a was determined to be 185°C and those of PBAF-a/6FDA alloy films were determined to be in the range of 210 - 260°C and the values are summarized in Table 5.2. The T_g values of the PBAF-a/6FDA alloy films were found to be much higher than PBAF-a and were observed to increase with the content of the dianhydride up to 2.5/1 mole ratio. The enhancement in T_g of PBAF-a/6FDA alloy films is attributed the tighter network formation by an additional ester linkage between phenolic hydroxyl group of PBAF-a and the anhydride group of 6FDA. In addition, the T_g values of the PBAF-a/6FDA alloy films at up to 1/1 mole ratio were found to be lower than that at 2.5/1 mole ratio. This was possibly due to an excess amount of dianhydride in the polymer alloy thus causing the network defects and lowering of network crosslink density.

5.5 Dynamic mechanical analyzer (DMA) study of 6FDA modified PBAF-a alloy films

The dynamic mechanical properties of PBAF-a and PBAF-a/6FDA alloy films and traditional polybenzoxazine (PBA-a) are illustrated in Figure 5.8 and the relevant values are summarized in Table 5.3. The PBAF-a and PBAF-a/6FDA alloy films showed only single glass transition temperature (T_g) as obtained from the maximum peak of loss modulus (E'') which corresponds to the initial drop from the glassy state to the transition state. The storage modulus (E') of PBAF-a/6FDA alloy films was higher than that of the PBAF-a due to the greater crosslink density of the PBAF-a/6FDA alloy films and the presence of the rigid structure of 6FDA in the polymer network. The

thermograms revealed the glassy state moduli, reported at room temperature (35°C) of the PBAF-a to be 1403 MPa and those of the PBAF-a/6FDA alloy films to be in the range of 1540 - 1864 MPa. The E' values clearly increased with increasing the 6FDA contents. Moreover, E' of PBAF-a/6FDA alloy films at 35°C presented a maximum value of PBAF-a/6FDA alloy film at 2.5/1 mole ratio. That is attributed to ultimate crosslink density and suitable amount of the anhydride at this blend ratio.

The T_g values from E'' of PBA-a and PBAF-a were approximately 160°C and 214°C, respectively. The T_g s of PBAF-a/6FDA alloy films were in the range of 250 - 287°C as displayed in Figure 5.9. From the figure, PBAF-a gives a higher T_g than PBA-a because PBAF-a has a more bulky group of hexafluoroisopropylidene $-(CF_3)_2-$ in its structure which led to the decrease in molecular mobility thus the lowering its free volume. In the same way, the decrease in molecular mobility or free volume leads to an increase in the T_g value. Moreover, an introduction of 6FDA into PBAF-a, which also contains hexafluoroisopropylidene $-(CF_3)_2-$ group, can substantially improve thermal stability of PBAF-a/6FDA alloy films. From the results, PBAF-a/6FDA alloy films provided the enhancement of crosslink density from additional ester linkage formation between phenolic hydroxyl group of the PBAF-a and the dianhydride group of 6FDA. The crosslink density of PBAF-a and PBAF-a/6FDA alloy films were calculated from the known rubbery plateau modulus values of the specimens using Neilsen's equation (equation (1)) and in the calculated values are tabulated in Table 5.3. The equation is

reported to effectively describe the elastic properties of dense network. Crosslink density (ρ_x) can be roughly estimated from the value of the equilibrium shear storage modulus in the rubbery region (E') which is equal to ($E'_e/3$) as the following [56];

$$\text{Log } E'_e/3 = 7.0 + 294\rho_x \quad (1)$$

where E'_e (dyne/cm²) is an equilibrium tensile storage modulus in rubbery plateau, ρ_x (mol/m³) is crosslink density (the mole number of network chains per unit volume)

The rubbery plateau modulus of PBAF-a/6FDA alloy films also increases when increasing the content of 6FDA with the highest value observed at PBAF-a/6FDA alloy film at 3/1 mole ratio while the alloy films of mole ratio at 2/1 and 1/1 showed the decrease of rubbery plateau due to an excess of 6FDA in the polymer alloy thus contributed to the network defects as discussed earlier.



5.6 Thermal stability of 6FDA modified PBAF-a alloy films

The thermal stability and decomposition of PBAF-a and PBAF-a/6FDA alloy films were determined using thermogravimetric analysis (TGA) under nitrogen atmosphere. Figure 5.11 and Figure 5.12 illustrate the weight loss curves of PBAF-a and PBAF-a/6FDA alloy films. The thermal stability of these samples were estimated by the decomposition temperature values at 5% and 10% weight loss (Td_5 and Td_{10}) and the char yield at 800°C. In this work, we are interested in Td_{10} and char yield and the

corresponding values are summarized in Table 5.4. $T_{d_{10}}$ and char yield for PBAF-a are 419°C and 58%. $T_{d_{10}}$ and char yield of BAF-a/6FDA were found to be in the range of 437 - 464°C and 50.0 - 57.3%. The TGA results show that the $T_{d_{10}}$ of PBAF-a/6FDA alloy films are higher than that of PBAF-a. The materials have the excellent thermal stability which was increased with increasing 6FDA content of PBAF-a/6FDA alloy films due to an attribution of the ester carbonyl linkage formation in PBAF-a/6FDA alloy films $T_{d_{10}}$ and char yield of PBAF-4fa are higher than the PBA-a due to the structures of PBAF-4fa containing the bulky CF_3 groups in structures which providing higher bond energy of C-F than C-H. Moreover, Figure 5.13 shows that DTG curves of PBA-a, PBAF-a and PBAF-a/6FDA alloy films in which, DTG weight loss of PBAF-a exhibited two stages at around 400 and 550°C which corresponded to the DTG weight loss of bisphenol-AF based poly(formal)s [57] and suggested the above temperature range in their DTG to be due to degradation of oxy-methylene bonds.

5.7 Thermal mechanical of 6FDA modified PBAF-a alloy films

Thermal mechanical analysis (TMA) is used to measure the coefficient of thermal expansion (CTE) of the materials using the tension probe to test the samples with an applied forced of 20mN. The TMA curves can be classified into two sections; first section has a linear section below T_g which almost reported the CTE of the material, the second section has a linear section above T_g . The T_g value is obtained from the change in slope between first and second sections. Table 5.5 and Figure 5.14 exhibit the

T_g and CTE values of PBAF-a and PBAF-a/6FDA alloy films. The T_g of PBAF-a and PBAF-a/6FDA alloy films at various mole ratios were found to be 180°C and 220 - 261°C of which the PBAF-a/6FDA alloy film at 3/1 mole ratio shows the highest T_g value. T_g values of all the alloy films shifted to higher temperature with the increase of 6FDA content. The linear section below T_g which defined the CTE of the PBAF-a and PBAF-a/6FDA alloy films in the range of 30 - 150°C were found to be 95 ppm/°C and 272 - 351 ppm/°C which are the CTE of each sample.

5.8 Dielectric constant of 6FDA modified PBAF-a alloy films

Dielectric constant indicates the ability of an insulator to store electrical energy. The dielectric constant value is directly related to the polarizability of the material, which measured by the parallel-plate capacitor method at 100 kHz. In comparison, the dielectric constant of the standard polyimide (Kapton) was measured to be in a range of 3.6 - 3.8 which is consistent with the value reported by the manufacturer [58]. The dielectric constant of PBA-a, PBAF-a and PBAF-a/6FDA alloy films are summarized Table 5.6. From the results, PBA-a and PBAF-a possess the dielectric constants of 3.71 and 3.24 respectively, in which non fluorine-containing benzoxazine expectedly shows a higher dielectric constant than fluorine-containing benzoxazine. The lower dielectric constant values can be explained by substitution of the hydrogen bond with F or hexafluoroisopropylidene (-CF₃) group which decreases the electric polarizability due

to strong electron with drawing inductive effect and trifluoromethyl group ($-CF_3$) is able to reduce the molecular packing and increased free volume [10, 59]. PBAF-a/6FDA alloy films at various ratio exhibit the decrease in dielectric constant values with increasing fluorine content in the structures similar to what observed in fluorine-containing polyimide [2].

5.9 Radius of curvature of 6FDA modified PBAF-a alloy films

Flexibility of the PBAF-a/6FDA alloy films can be tested by bending the alloy films at different radius of curvature. Figure 5.15 illustrates the films having a dimension of 1 cm × 5 cm × 0.01 cm and the bending test was performed using the forceps to clamp each film specimen at the positions of 0.2 cm to 2 cm as seen in figure. The smallest radius of curvature of the films before breaking was then recorded as displayed in Figure 5.16 and summarized in Table 5.7. It can be seen that PBAF-a/6FDA alloys film at 2.5/1 mole ratio exhibits the lowest radius of curvature compared to the other PBAF-a/6FDA alloy films which indicated that the PBAF-a/6FDA alloy film at 2.5/1 mole ratio is the most flexible films compared to the other alloy compositions. This is due to the networks of the 2.5/1 alloys film has the highest crosslink density from the highest ester linkage formation in the network. This ester linkage is more flexible in nature than the Mannich bridge and other linkages in traditional polybenzoxazine network.

5.10 Contact angle of 6FDA modified PBAF-a alloy films

Contact angle is indicative of a hydrophobic or hydrophilic behavior of materials. The images in Figure 5.17 show water contact angle (θ_w) of PBA-a and PBAF-a to be 72.4° and 92.9°, respectively whereas PBAF-a/6FDA alloy films provide the values to be in a range of 75.9° - 99.4°. All data are plotted in Figure 5.18 and summarized in Table 5.8. It is evident that the fluorine-containing polybenzoxazine shows relatively high hydrophobic behavior. The water contact angle of PBAF-a is greater than PBA-a as the fluorine atom is bigger than the hydrogen atom and incorporated the bulky CF_3 groups with a hemispherical volume of 42.6 Å³ which increased the chemical group size. Therefore, the $-\text{CF}_3$ group covers the surface to greater extent than $-\text{CH}_3$ group with a volume of 16.8 Å³ and minimizes the interaction of water with any underlying polar groups [60]. The values of water contact angle for PBAF-a/6FDA alloy films were increased with the increase of the fluorine content. However, the water contact angle of PBAF-a was higher than PBAF-a/6FDA alloy films at 2/1 mole ratio to 5/1 mole ratio. For this reason, PBAF-a may be attributed the free network formation of polybenzoxazine. Moreover, the water contact angle of polytetrafluoroethylene (Teflon) which has the fluorine atoms in the structure is reported to be the range of 106 - 121°[61].

5.11 Solvent extraction of 6FDA modified PBAF-a alloy films

The solvent extraction of 6FDA modified PBAF-a alloy films at various mole ratios after completely cured at 240°C was performed using chloroform as a common solvent at room temperature. The solvent extraction results were obtained by measuring the weight of samples and calculating the percent extraction after 30 days in chloroform and the resulting values were summarized in Table 5.9. From the table, all samples provided the percent extraction in the solvent of less than 1% suggesting infinite network formation to be achieved in all specimens under this investigation.



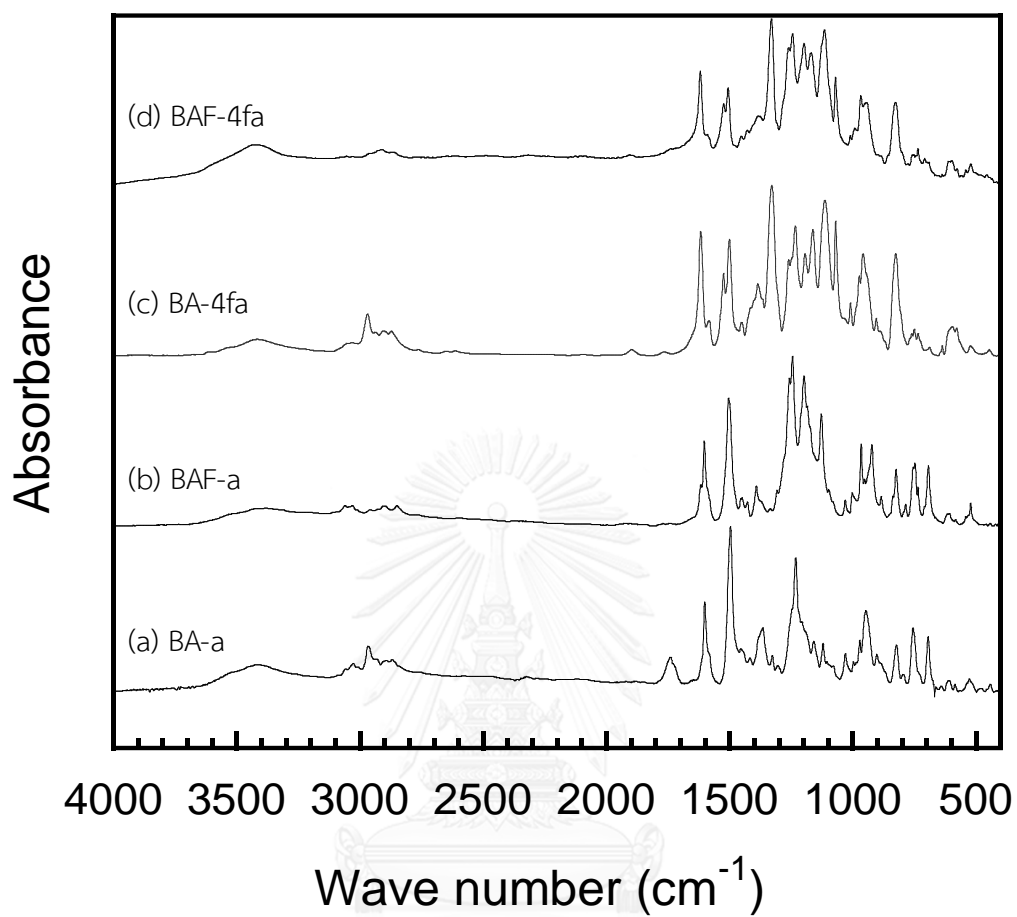


Figure 5.3 FTIR spectra of benzoxazine monomers: (a) BA-a, (b) BAF-a, (c) BA-4fa and (d) BAF-4fa

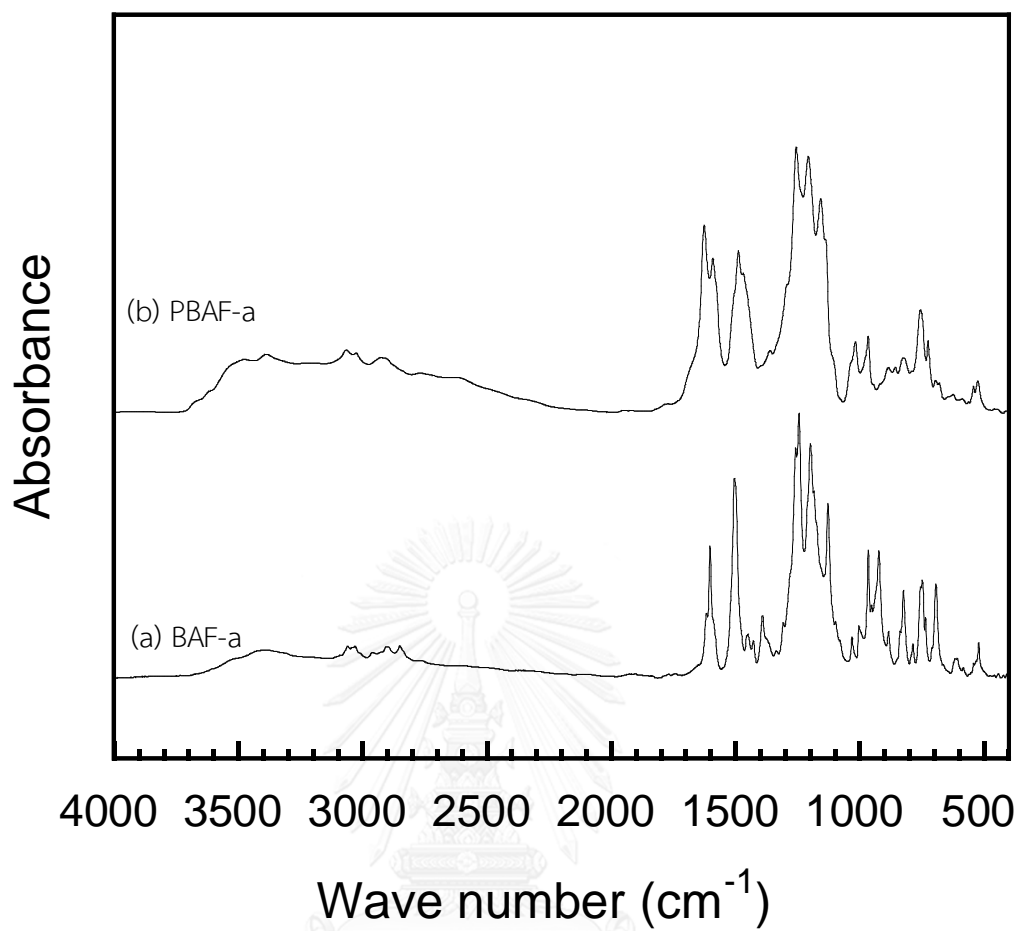


Figure 5.4 FTIR spectra of fluorine-containing benzoxazine monomer (a) BAF-a and fluorine-containing polybenzoxazine (b) PBAF-a.

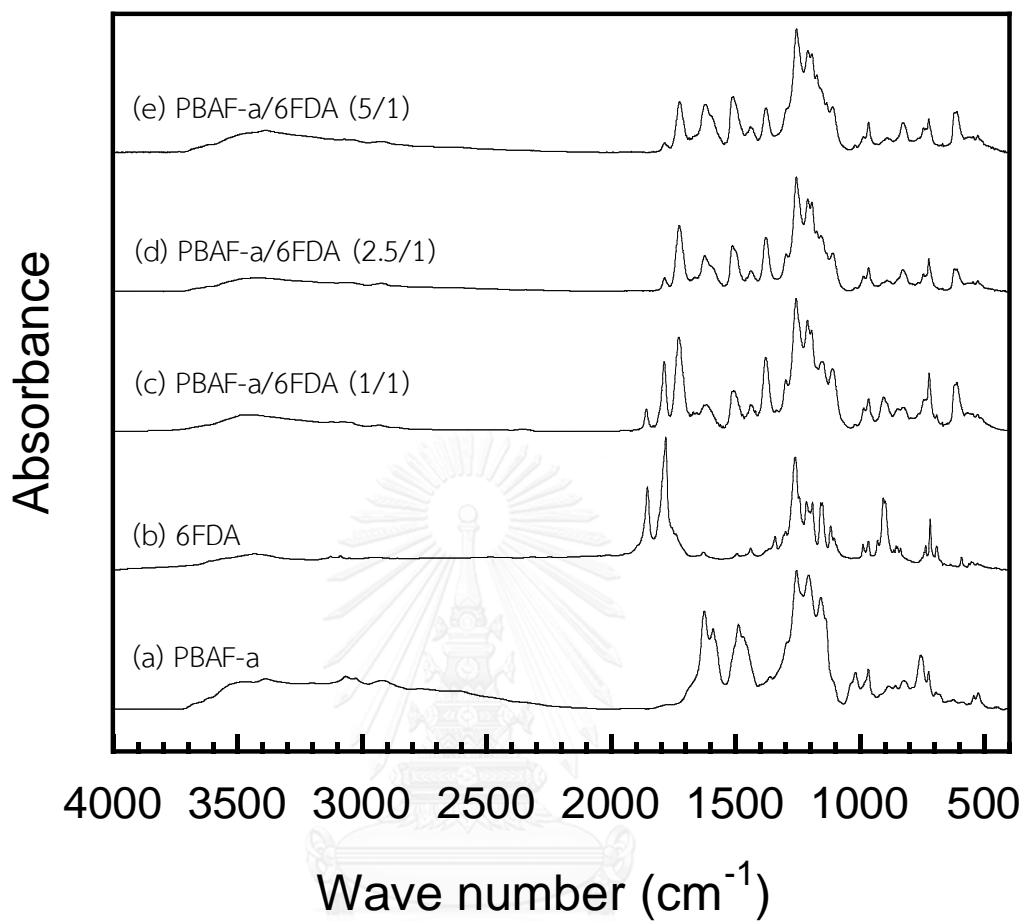


Figure 5.5 FTIR spectra of (a) PBA-a, (b) 6FDA, (c) PBAF-a/6FDA 1/1, (d) PBAF-a/6FDA 2.5/1 and (e) PBAF-a/6FDA 5/1.

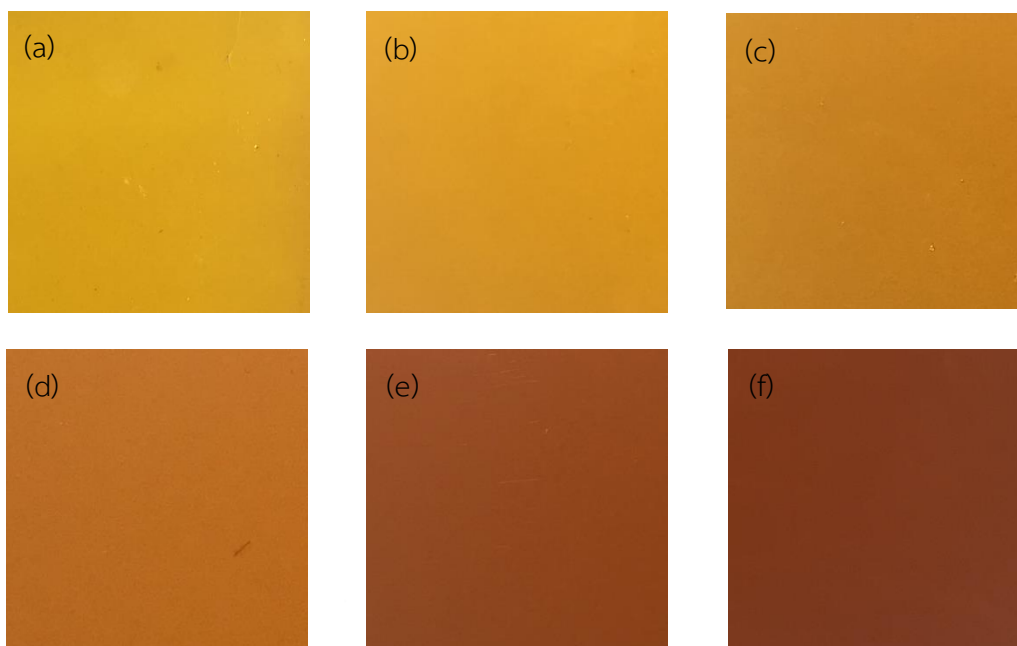


Figure 5.6 The appearance color of PBAF-a/6FDA at various ratios (a) PBAF-a/6FDA 1/1, (b) PBAF-a/6FDA 2/1, (c) PBAF-a/6FDA 2.5/1, (d) PBAF-a/6FDA 3/1, (e) PBAF-a/6FDA 4/1 and (f) PBAF-a/6FDA 5/1.

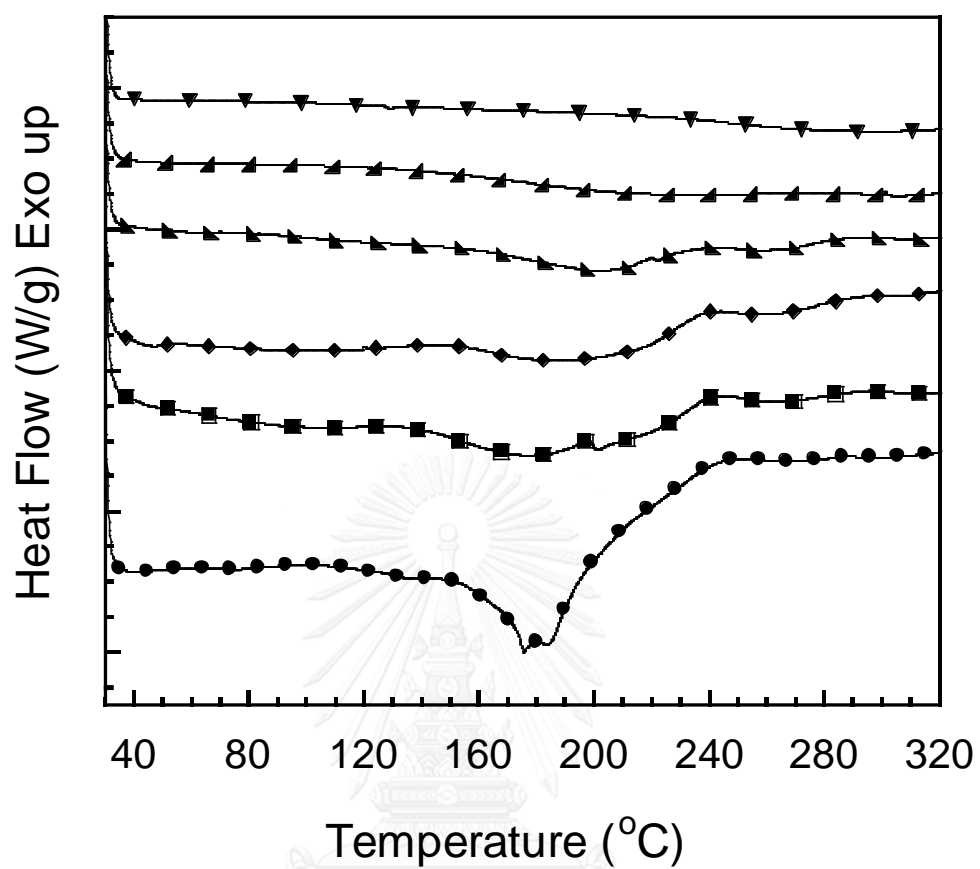


Figure 5.7 DSC thermograms of fluorine-containing benzoxazine blending with 6FDA at 2.5/1 mole ratio at various conditions: (●) 80°C 1 h, (■) 130°C 1 h, (◆) 150°C /1 h, (▴) 170°C /1 h, (▾) 210°C /1 h and (▼) 240°C /2 h.

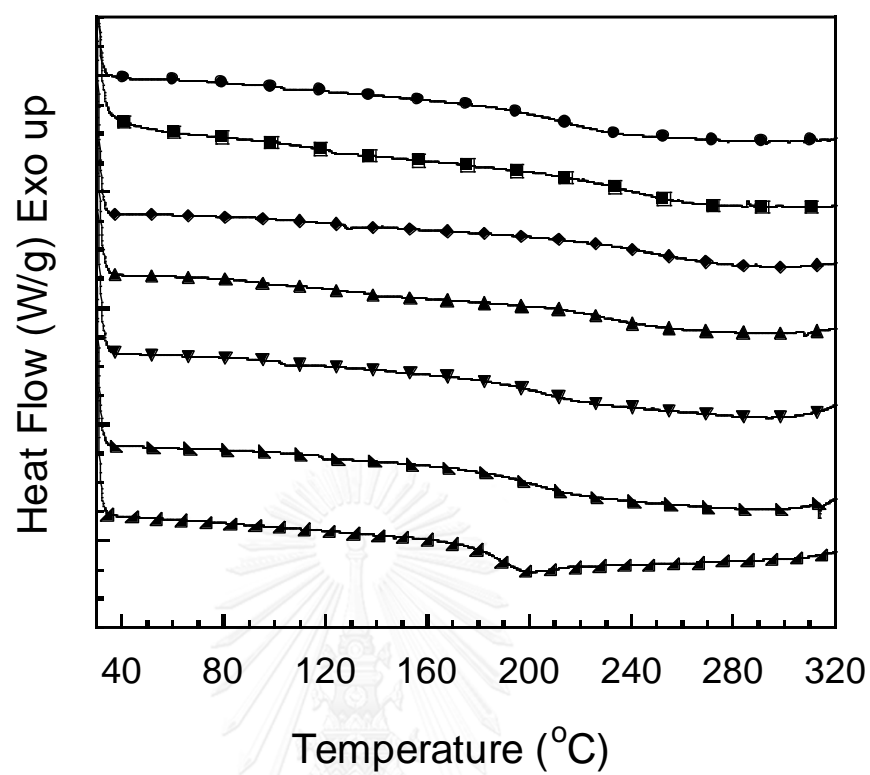


Figure 5.8 DSC thermograms of PBAF-a/6FDA at various mole ratios: (●) PBAF-a/6FDA 1/1, (■) PBAF-a/6FDA 2/1, (◆) PBAF-a/6FDA 2.5/1, (▲) PBAF-a/6FDA 3/1, (▼) PBAF-a/6FDA 4/1, (▴) PBAF-a/6FDA 5/1 and (▲) PBAF-a.

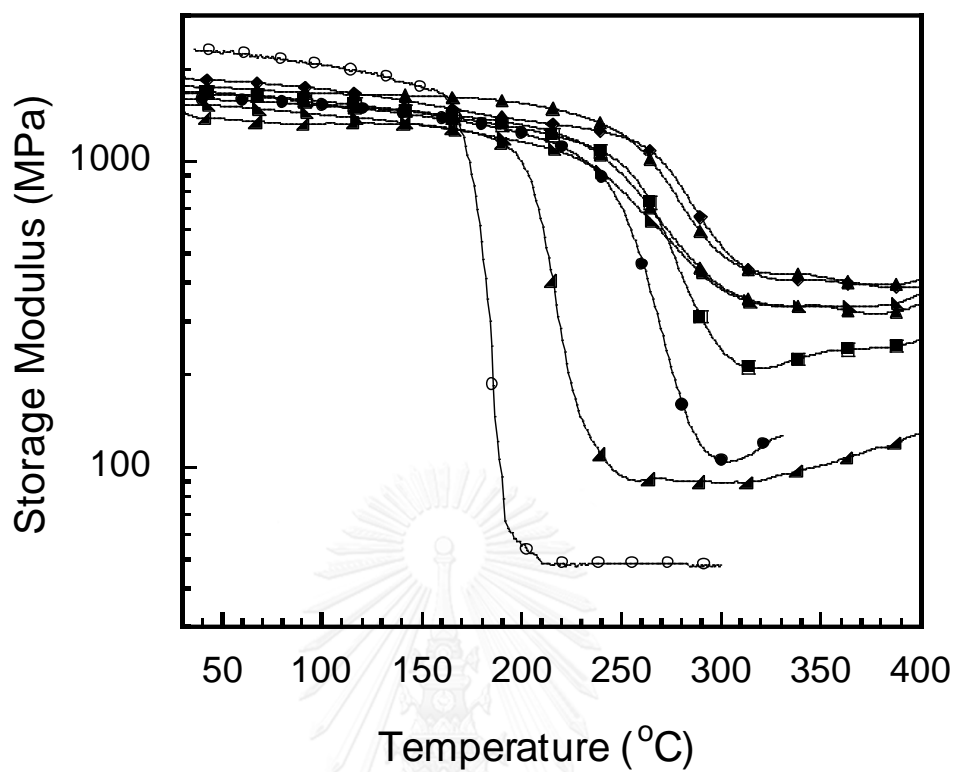


Figure 5.9 Storage modulus of PBAF-a/6FDA at various mole ratios: (●) PBAF-a/6FDA 1/1, (■) PBAF-a/6FDA 2/1, (◆) PBAF-a/6FDA 2.5/1, (▲) PBAF-a/6FDA 3/1, (▼) PBAF-a/6FDA 4/1, (▴) PBAF-a/6FDA 5/1, (▴) PBAF-a and (○) PBA-a.

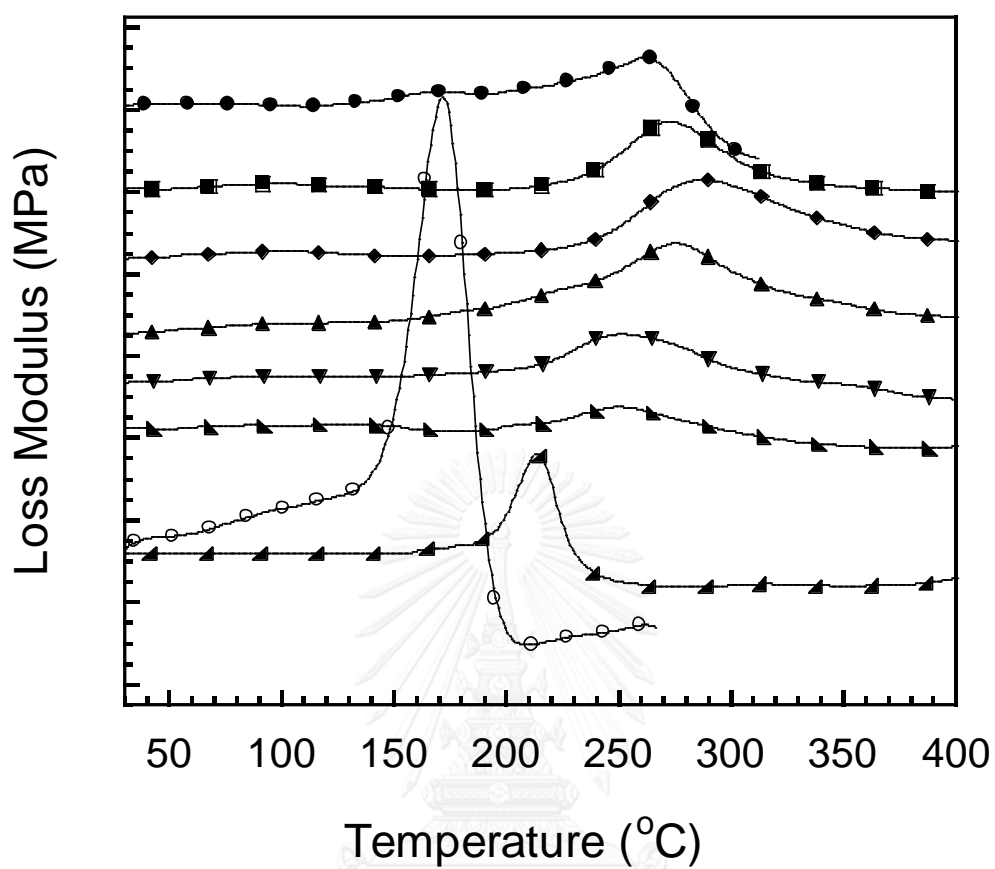


Figure 5.10 Loss modulus of PBAF-a/6FDA at various mole ratios: (●) PBAF-a/6FDA 1/1, (■) PBAF-a/6FDA 2/1, (◆) PBAF-a/6FDA 2.5/1, (▲) PBAF-a/6FDA 3/1, (▼) PBAF-a/6FDA 4/1, (▲) PBAF-a/6FDA 5/1, (▲) PBAF-a and (O) PBA-a.

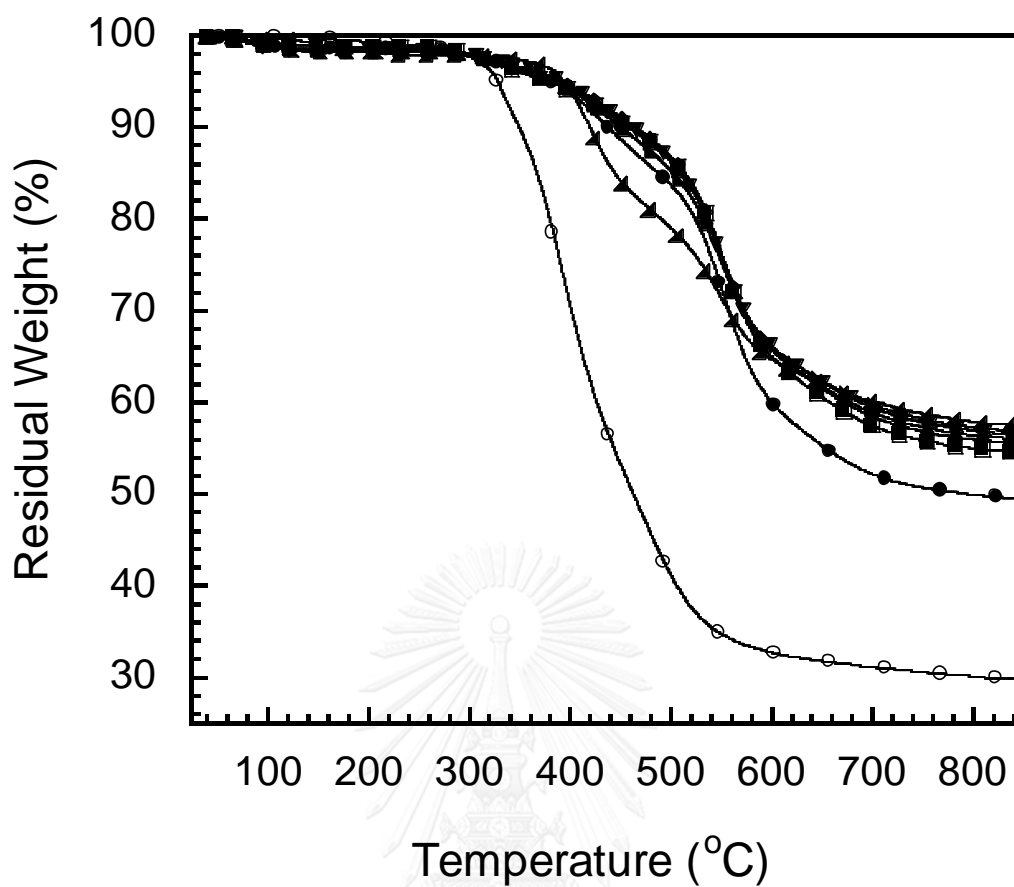


Figure 5.11 Thermal degradation PBAF-a/6FDA at various mole ratios: (●) PBAF-a/6FDA 1/1, (■) PBAF-a/6FDA 2/1, (◆) PBAF-a/6FDA 2.5/1, (▲) PBAF-a/6FDA 3/1, (▼) PBAF-a/6FDA 4/1, (▴) PBAF-a/6FDA 5/1, (▲) PBAF-a and (○) PBA-a.

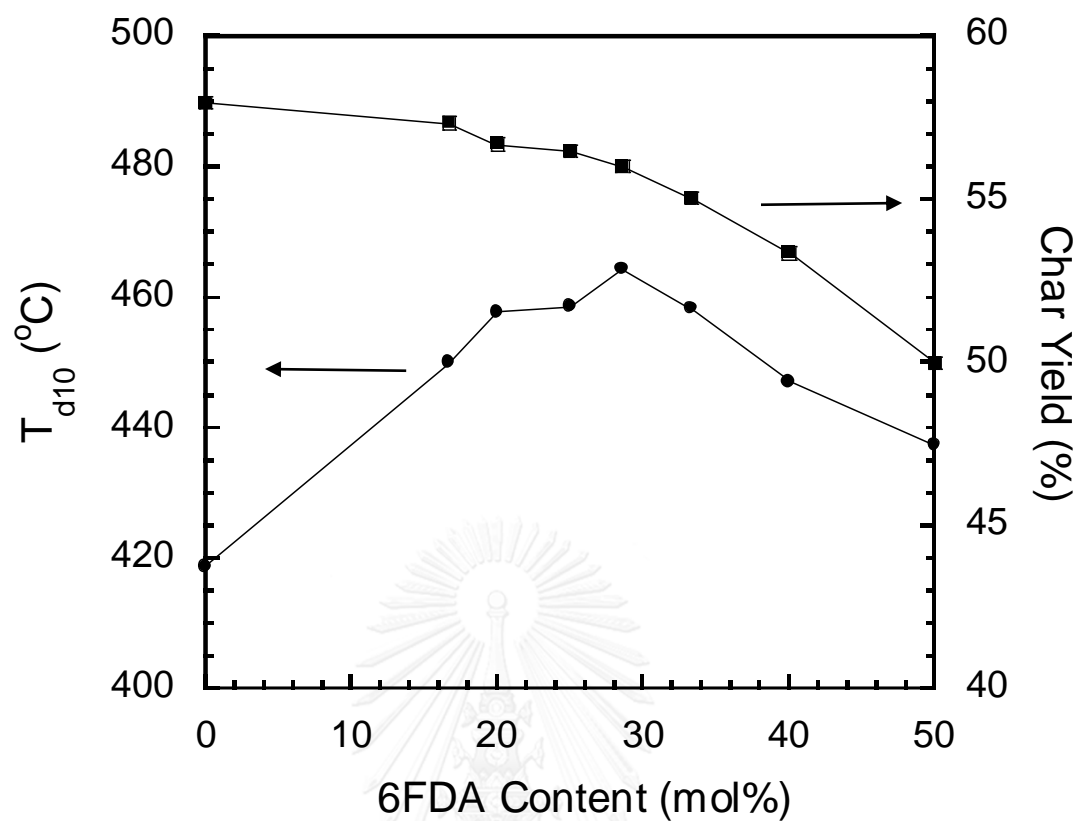


Figure 5.12 Thermal degradation temperature at 10% weight loss and char yield of

PBAF-a/6FDA at various 6FDA content.

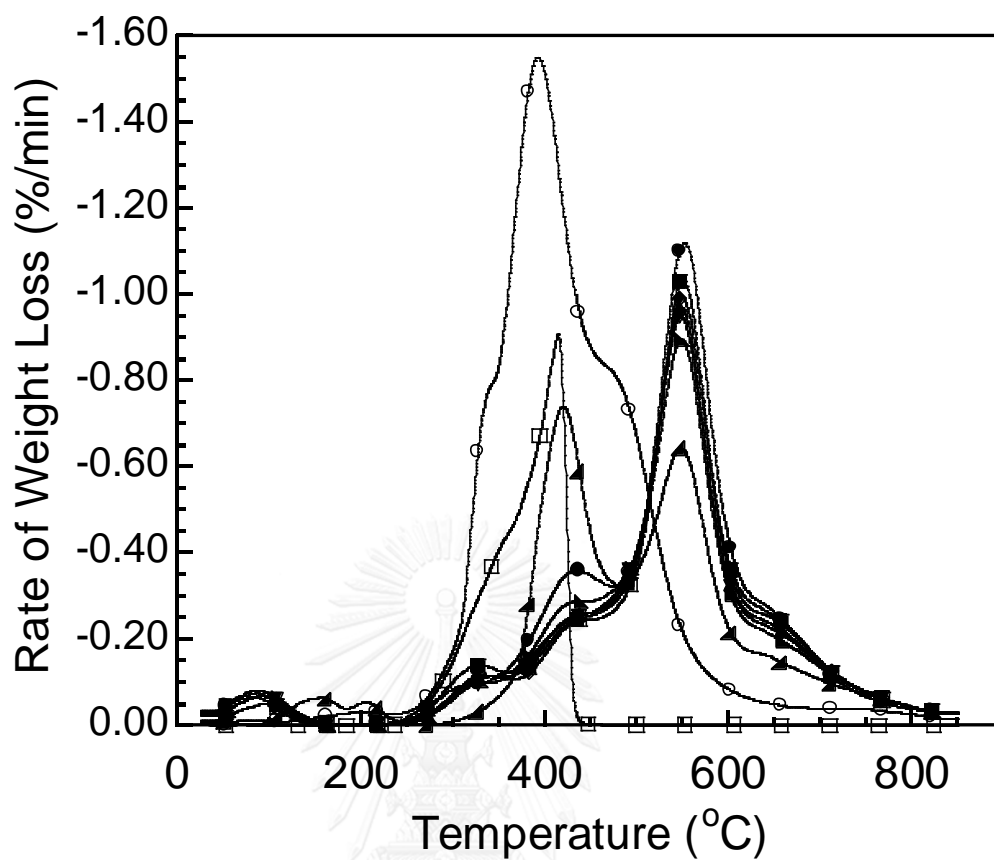


Figure 5.13 Rate of weight loss PBAF-a/6FDA at various mole ratios: (●) PBAF-a/6FDA 1/1, (■) PBAF-a/6FDA 2/1, (◆) PBAF-a/6FDA 2.5/1, (▲) PBAF-a/6FDA 3/1, (▼) PBAF-a/6FDA 4/1, (▴) PBAF-a/6FDA 5/1, (▲) PBAF-a, (○) PBA-a and (□) 6FDA.

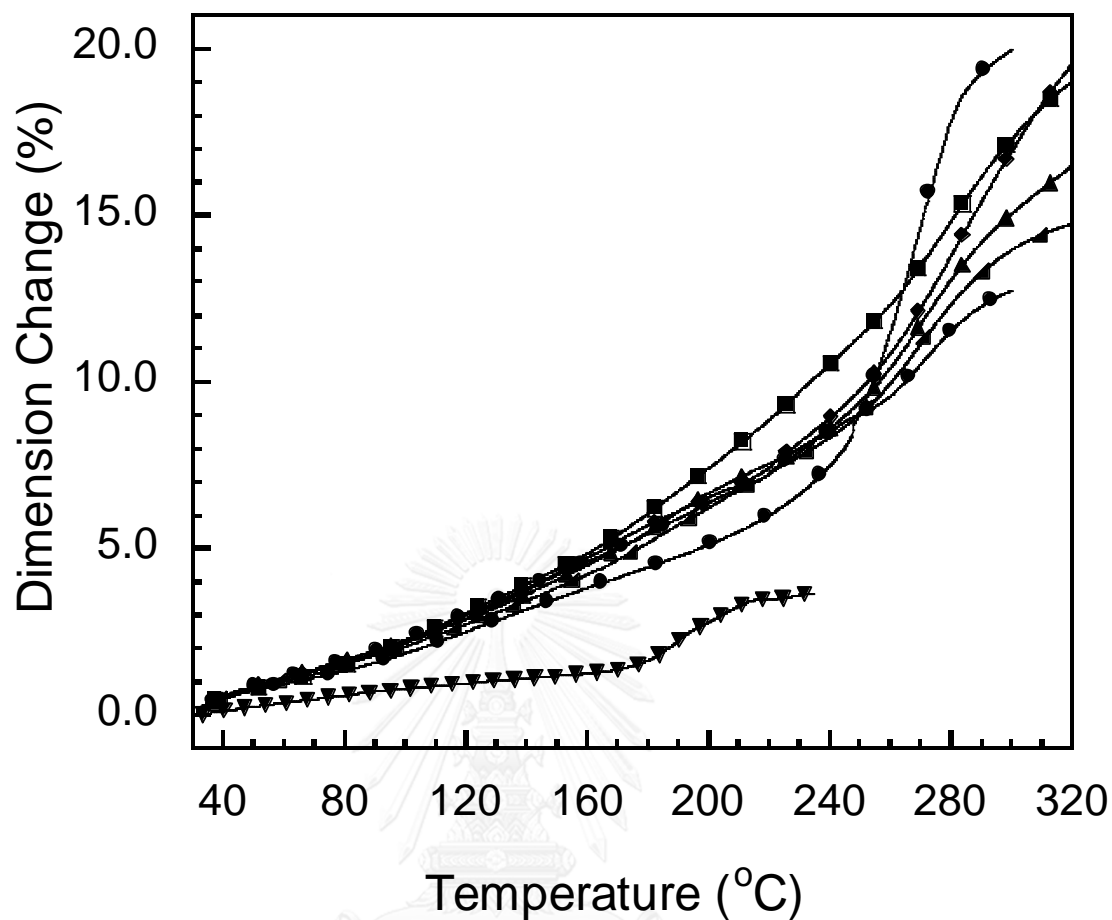


Figure 5.14 TMA curves of PBAF-a/6FDA at various mole ratios: (●) PBAF-a/6FDA 1/1, (■) PBAF-a/6FDA 2/1, (◆) PBAF-a/6FDA 2.5/1, (▲) PBAF-a/6FDA 3/1, (▼) PBAF-a/6FDA 4/1, (▴) PBAF-a/6FDA 5/1 and (◄) PBAF-a.

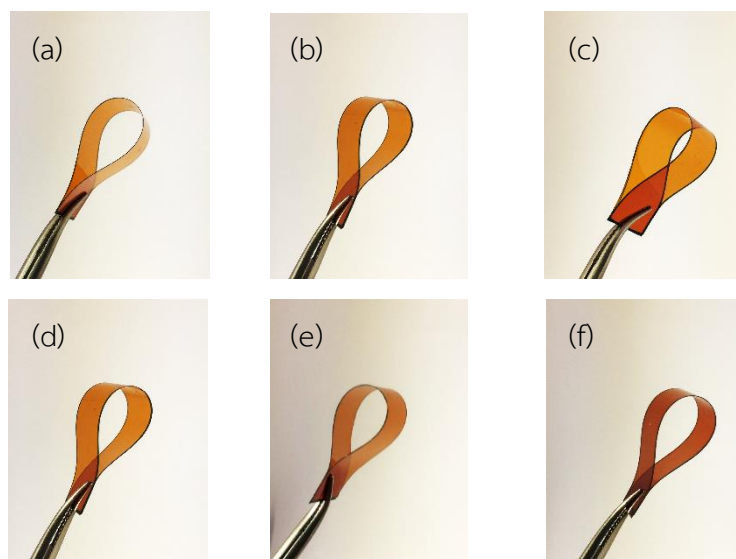
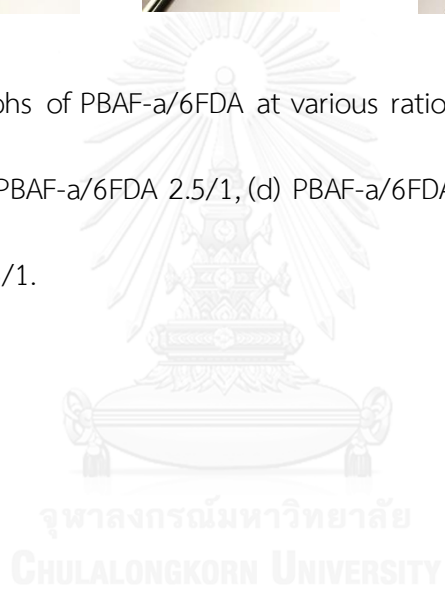


Figure 5.15 Photographs of PBAF-a/6FDA at various ratios: (a) PBAF-a/6FDA 1/1, (b) PBAF-a/6FDA 2/1, (c) PBAF-a/6FDA 2.5/1, (d) PBAF-a/6FDA 3/1, (e) PBAF-a/6FDA 4/1 and (f) PBAF-a/6FDA 5/1.



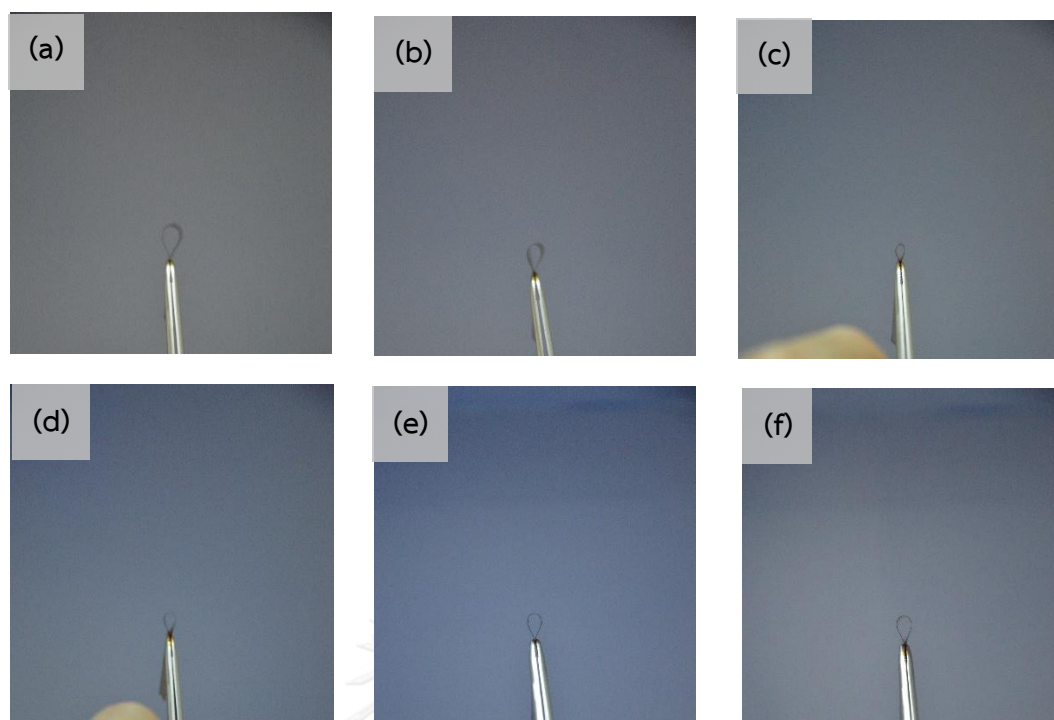


Figure 5.16 The optimum radius of curvature of PBAF-a/6FDA at various ratios:

(a) PBAF-a/6FDA 1/1, (b) PBAF-a/6FDA 2/1, (c) PBAF-a/6FDA 2.5/1, (d) PBAF-a/6FDA 3/1, (e) PBAF-a/6FDA 4/1 and (f) PBAF-a/6FDA 5/1.

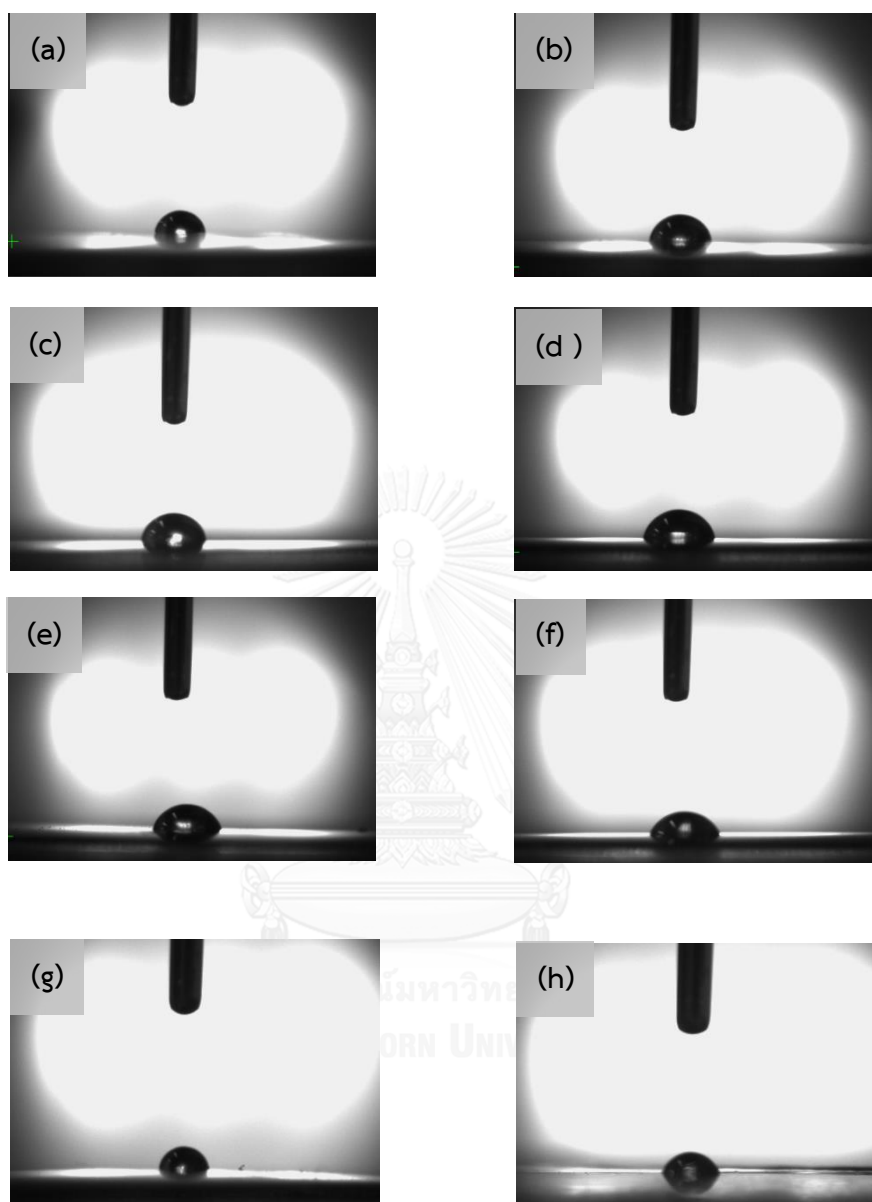


Figure 5.17 Appearance of water contact angle of PBAF-a/6FDA at various mole ratios:

- (a) PBAF-a/6FDA 1/1, (b) PBAF-a/6FDA 2/1, (c) PBAF-a/6FDA 2.5/1, (d) PBAF-a/6FDA 3/1, (e) PBAF-a/6FDA 4/1, (f) PBAF-a/6FDA 5/1, (g) PBAF-a and (h) PBA-a.

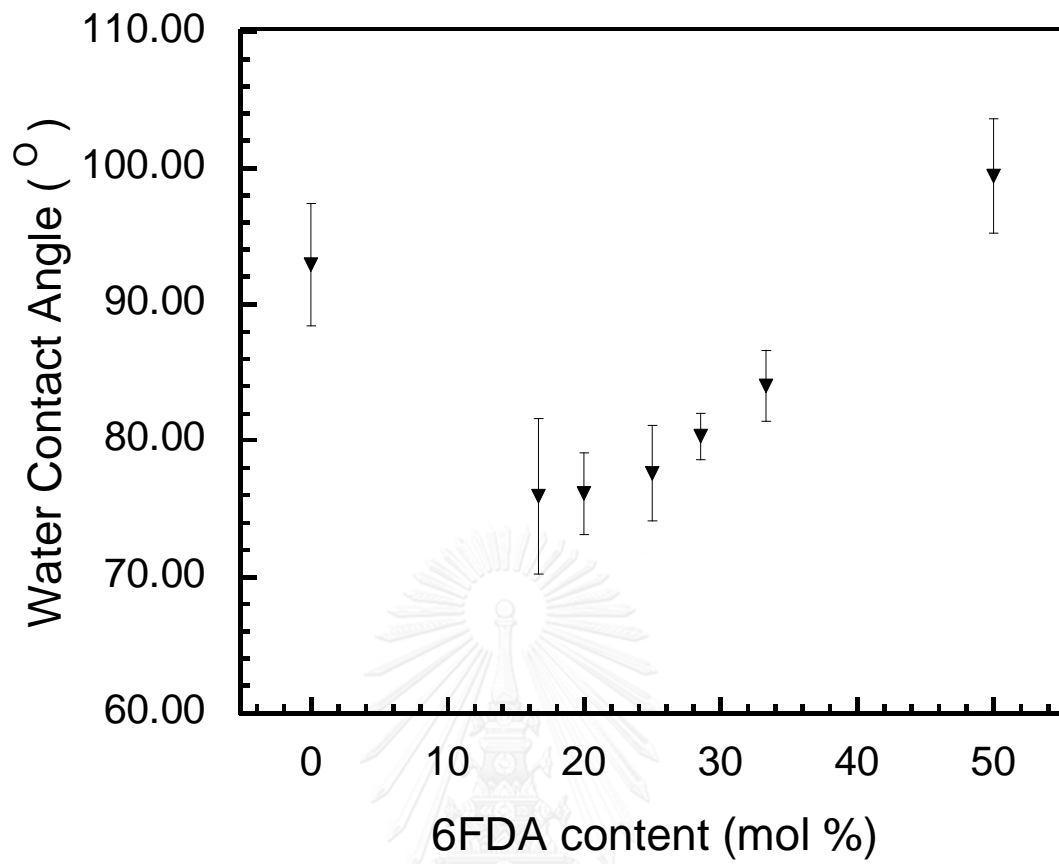


Figure 5.18 Water contact angle of PBAF-a/6FDA at various 6FDA content.

Table 5.1 Summarize of thermogravimetric analysis data of polybenzoxazine/6FDA alloy films

TGA Properties	Ratio (Benzoxazine/6FDA) or 6FDA content		Matrix			
			PBA- a/6FDA	PBA- 4fa/6FDA	PBAF- a/6FDA	PBAF- 4fa/6FDA
Td ₅ (°C)	Pure	0.00	328	317	393	379
	5/1	16.67	346	367	385	389
	4/1	20.00	348	360	385	387
	3/1	25.00	349	361	387	375
	2.5/1	28.57	338	368	388	371
	2/1	33.33	364	361	379	373
	1.5/1	40.00	368	365	371	364
	1/1	50.00	398	355	382	366
Td ₁₀ (°C)	Pure	0.00	349	360	419	453
	5/1	16.67	381	436	450	465
	4/1	20.00	386	419	458	461
	3/1	25.00	386	416	459	444
	2.5/1	28.57	387	418	464	417
	2/1	33.33	399	399	458	415
	1.5/1	40.00	405	401	447	393
	1/1	50.00	423	383	437	398
Char yield	Pure	0.00	30.1	57.9	58.0	53.1
	5/1	16.67	49.9	57.4	57.3	52.8
	4/1	20.00	50.3	55.4	56.7	53.3
	3/1	25.00	49.4	54.9	56.5	49.5
	2.5/1	28.57	53.0	53.4	56.0	47.7
	2/1	33.33	49.5	48.7	55.1	46.2
	1.5/1	40.00	50.6	46.1	53.4	41.4
	1/1	50.00	49.6	36.8	50.0	43.5

Table 5.2 Glass transition temperature (T_g) of fluorine-containing benzoxazine and their PBAF-a/6FDA alloy films at various mole ratios

Ratio (PBAF-a/6FDA)	6FDA content (%)	Glass transition temperature (°C)
PBAF-a	0.00	185
5/1	16.7	203
4/1	20.0	211
3/1	25.0	230
2.5/1	28.6	260
2/1	33.3	240
1/1	50.0	220

Table 5.3 Glass transition temperature from loss modulus (E''), storage modulus (E') at room temperature (35°C), storage modulus at rubbery plateau (E') and crosslink density of fluorine-containing benzoxazine and PBAF-a/6FDA alloy films at various mole ratios which were determined by DMA

Ratio (PBAF-a/6FDA)	6FDA content (%)	T_g from E'' ($^\circ\text{C}$)	Storage modulus at 35°C (MPa)	Storage modulus (E') at rubbery plateau (MPa)	Crosslink density (mol/m^3)
PBA-a	0.00	168	2305	48	4109.6
PBAF-a	0.00	214	1403	91	5057.7
5/1	16.7	250	1540	335	6989.5
4/1	20.0	255	1671	337	6998.3
3/1	25.0	275	1759	428	7352.6
2.5/1	28.6	287	1864	410	7289.0
2/1	33.3	272	1698	211	6304.3
1/1	50.0	262	1593	98	5167.6

Table 5.4 Degradation temperature at 5% weight loss (T_{d5}), Degradation temperature at 10% weight loss (T_{d10}), residue weight (char yield) at 800°C and LOI of fluorine-containing benzoxazine and PBAF-a/6FDA alloy films at various mole ratios

Ratio (PBAF-a/6FDA)	6FDA content (%)	T_{d5} (°C)	T_{d10} (°C)	Char Yield (%)	LOI
PBA-a	0.00	327	349	30.1	29.5
PBAF-a	0.00	393	419	58.0	40.7
5/1	16.7	385	450	57.3	40.4
4/1	20.0	385	458	56.7	40.1
3/1	25.0	387	459	56.5	40.1
2.5/1	28.6	388	464	56.0	39.9
2/1	33.3	379	458	55.1	39.5
1/1	50.0	382	437	50.0	37.5

Table 5.5 Glass transition temperature (T_g) from TMA and coefficient of thermal expansion of fluorine-containing benzoxazine and their PBAF-a/6FDA alloy films at various mole ratios

Ratio (PBAF-a/6FDA)	6FDA content (%)	Glass transition temperature ($^{\circ}\text{C}$)	Coefficient of thermal expansion ($\text{ppm}/^{\circ}\text{C}$)
PBAF-a	0.00	180	95
5/1	16.7	225	326
4/1	20.0	235	336
3/1	25.0	266	351
2.5/1	28.6	261	301
2/1	33.3	252	334
1/1	50.0	220	272



Table 5.6 Dielectric constants of fluorine-containing benzoxazine and PBAF/a:6FDA alloy films at various mole ratios

Ratio (PBAF-a/6FDA)	6FDA content (%)	Dielectric constant
PBA-a	0.00	3.71 ± 0.04
PBAF-a	0.00	3.24 ± 0.06
5/1	16.7	3.11 ± 0.07
4/1	20.0	2.99 ± 0.06
3/1	25.0	2.88 ± 0.04
2.5/1	28.6	2.84 ± 0.05
2/1	33.3	2.77 ± 0.05
1/1	50.0	2.61 ± 0.06

Table 5.7 Radius of curvature of PBAF-a/6FDA alloy films at various mole ratios

Ratio (PBAF-a/6FDA)	6FDA content (%)	Radius (cm)	Diameter (cm)	Arc Length (cm)
PBAF-a	0.00	0.0	0.00	0.00
5/1	16.7	0.15	0.30	0.50
4/1	20.0	0.15	0.30	0.50
3/1	25.0	0.15	0.30	0.50
2.5/1	28.6	0.10	0.20	0.30
2/1	33.3	0.20	0.40	0.60
1/1	50.0	0.28	0.55	0.90

Table 5.8 Contact angle and surface free energy of fluorine-containing benzoxazine and PBAF-a/6FDA alloy films at various mole ratios

Ratio (PBAF-a/6FDA)	6FDA content (%)	Water Contact angle (°)
PBA-a	0.00	72.4 ± 5.8
PBAF-a	0.00	92.9 ± 4.5
5/1	16.7	75.9 ± 5.7
4/1	20.0	76.1 ± 3.0
3/1	25.0	77.6 ± 3.5
2.5/1	28.6	80.3 ± 1.7
2/1	33.3	84.0 ± 2.6
1/1	50.0	99.4 ± 4.2

Table 5.9 Solvent extraction data at various mole ratios of 6FDA modified PBA-a alloy films

Ratio (PBAF-a/6FDA)	6FDA content (%)	Mass of specimen (mg)					Percent extraction (%)
		Initial	1 week	2 week	3 week	4 week	
PBAF-a	0.00	88.4	88.0	88.0	87.9	87.9	0.56
5/1	16.7	51.7	51.6	51.6	51.6	51.5	0.38
4/1	20.0	40.4	40.3	40.3	40.3	40.3	0.24
3/1	25.0	47.7	47.7	47.6	47.6	47.6	0.21
2.5/1	28.6	61.9	61.7	61.7	61.7	61.7	0.16
2/1	33.3	53.9	53.9	53.6	53.6	53.6	0.55
1/1	50.0	37.7	37.6	37.6	37.5	37.4	0.79



CHAPTER VI

CONCLUSIONS

A novel fluorine-containing benzoxazine monomers with three types i.e. BA-4fa, BAF-a and BAF-4fa have been successfully synthesized by solventless method. The functional groups of fluorine-containing benzoxazine monomers were supported and confirmed by FTIR spectra.

PBAF-a/6FDA alloy film provided the highest T_{d10} and char yield at 800°C than PBA-a/6FDA, PBA-4fa/6FDA and PBAF-4fa/6FDA.

The network formation of carbonyl ester linkage (-COO-) between phenolic hydroxyl group of polybenzoxazine and carbonyl group of dianhydride was confirmed by FTIR spectra which can enhanced the flexibility of alloy films.

The fluorine-containing polybenzoxazine possessed excellent thermal stability, low dielectric constant and high water contact angle compared to non fluorine-containing polybenzoxazine.

PBAF-a/6FDA alloy film at 2.5/1 mole ratio exhibited the excellent thermal stability properties (T_g and T_d) and physical properties (water contact angle and flexibility).

PBAF-a/6FDA alloy films are appropriate for an application as polymeric film for coating and high thermal resistant material.

REFERENCES

- [1] Ebnesajjad, S. and Morgan, R.A., Fluoropolymer Additives. 2012, Oxford: William Andrew.
- [2] Ghosh, M.K. and Mittal, K.L., Polyimides: Fundamentals and Applications 1996, New York: Marcel Dekker.
- [3] Ebnesajjad, S. and Khaladkar, P.R., Fluoropolymers applications in chemical processing industries. 2005, New York: William Andrew.
- [4] Dodiuk, H. and Goodman, S.H., Handbook of Thermoset Plastics. 3rd ed. 2014, California: William Andrew.
- [5] Ge, Z.Y., Tao, Z.Q., Li, G., Ding, J.P., Fan, L., and Yang, S.Y., Synthesis and properties of novel fluorinated epoxy resins. Journal of Applied Polymer Science, 2011. 120(1): p. 148-155.
- [6] Tao, Z., Yang, S., Ge, Z., Chen, J., and Fan, L., Synthesis and properties of novel fluorinated epoxy resins based on 1,1-bis(4-glycidylesterphenyl)-1-(3'-trifluoromethylphenyl)-2,2,2-trifluoroethane. European Polymer Journal, 2007. 43(2): p. 550-560.
- [7] Damaceanu, M.-D., Constantin, C.-P., Nicolescu, A., Bruma, M., Belomoina, N., and Begunov, R.S., Highly transparent and hydrophobic fluorinated polyimide films with ortho-kink structure. European Polymer Journal, 2014. 50(0): p. 200-213.
- [8] Şen, F. and Kahraman, M.V., Preparation and properties of nano diamond/6F-bisphenol A-based cyanate ester composites. Polymer Composites, 2013. 34(12): p. 1977-1985.
- [9] Lin, C.H., Chang, S.L., Lee, H.H., Chang, H.C., Hwang, K.Y., Tu, A.P., and Su, W.C., Fluorinated benzoxazines and the structure-property relationship of resulting polybenzoxazines. Journal of Polymer Science Part A: Polymer Chemistry, 2008. 46(15): p. 4970-4983.

- [10] Su, Y.-C. and Chang, F.-C., Synthesis and characterization of fluorinated polybenzoxazine material with low dielectric constant. Polymer, 2003. 44(26): p. 7989-7996.
- [11] wikipedia. *Crystallization of polymers*. 2014 [cited 2014 11 Sep]; Available from: http://en.wikipedia.org/wiki/Crystallization_of_polymers.
- [12] Ishida, H. and Agag, T., Handbook of benzoxazine resin. 2011, Oxford: Elsevier.
- [13] Takeichi, T., Kawauchi, T., and Agag, T., High Performance Polybenzoxazines as a Novel Type of Phenolic Resin. Polym. J, 2008. 40(12): p. 1121-1131.
- [14] Rimdusit, S., Tiptipakorn, S., Jubsilp, C., and Takeichi, T., Polybenzoxazine alloys and blends: Some unique properties and applications. Reactive and Functional Polymers, 2013. 73(2): p. 369-380.
- [15] Takeichi, T., Kano, T., and Agag, T., Synthesis and thermal cure of high molecular weight polybenzoxazine precursors and the properties of the thermosets. Polymer, 2005. 46(26): p. 12172-12180.
- [16] Takeichi, T., Guo, Y., and Rimdusit, S., Performance improvement of polybenzoxazine by alloying with polyimide: effect of preparation method on the properties. Polymer, 2005. 46(13): p. 4909-4916.
- [17] Liu, Y., Yue, Z., and Gao, J., Synthesis, characterization, and thermally activated polymerization behavior of bisphenol-S/aniline based benzoxazine. Polymer, 2010. 51(16): p. 3722-3729.
- [18] Wang, J., Fang, X., Wu, M.-q., He, X.-y., Liu, W.-b., and Shen, X.-d., Synthesis, curing kinetics and thermal properties of bisphenol-AP-based benzoxazine. European Polymer Journal, 2011. 47(11): p. 2158-2168.
- [19] Rimdusit, S., Mongkhonsi, T., Kamonchaivanich, P., Sujirote, K., and Thiptipakorn, S., Effects of polyol molecular weight on properties of benzoxazine-urethane polymer alloys. Polymer Engineering & Science, 2008. 48(11): p. 2238-2246.
- [20] Rimdusit, S., Kunopast, P., and Dueramae, I., Thermomechanical properties of arylamine-based benzoxazine resins alloyed with epoxy resin. Polymer Engineering & Science, 2011. 51(9): p. 1797-1807.

- [21] Jubsilp, C., Takeichi, T., and Rimdusit, S., Property enhancement of polybenzoxazine modified with dianhydride. Polymer Degradation and Stability, 2011. 96(6): p. 1047-1053.
- [22] Rimdusit, S., Ramsiri, B., Jubsilp, C., and Dueramae, I., Characterizations of polybenzoxazine modified with isomeric biphenyltetracarboxylic dianhydrides. Express Polymer Letters, 2012. 6(10): p. 773-782.
- [23] Jubsilp, C., Ramsiri, B., and Rimdusit, S., Effects of aromatic carboxylic dianhydrides on thermomechanical properties of polybenzoxazine-dianhydride copolymers. Polymer Engineering & Science, 2012. 52(8): p. 1640-1648.
- [24] Jang, W., Shin, D., Choi, S., Park, S., and Han, H., Effects of internal linkage groups of fluorinated diamine on the optical and dielectric properties of polyimide thin films. Polymer, 2007. 48(7): p. 2130-2143.
- [25] Maier, G., Low dielectric constant polymers for microelectronics. Progress in Polymer Science, 2001. 26(1): p. 3-65.
- [26] Choi, I.H. and Chang, J.-H., Colorless polyimide nanocomposite films containing hexafluoroisopropylidene group. Polymers for Advanced Technologies, 2011. 22(5): p. 682-689.
- [27] Wang, C.-Y., Zhao, H.-P., Li, G., and Jiang, J.-M., Novel fluorinated polyimides derived from an unsymmetrical diamine containing trifluoromethyl and methyl pendant groups. Polymers for Advanced Technologies, 2011. 22(12): p. 1816-1823.
- [28] Jang, W., Lee, H.-S., Lee, S., Choi, S., Shin, D., and Han, H., The optical and dielectric characterization of light-colored fluorinated polyimides based on 1,3-bis(4-amino-2-trifluoromethylphenoxy)benzene. Materials Chemistry and Physics, 2007. 104(2-3): p. 342-349.
- [29] Ishida, H., *Process for preparation of benzoxazine compounds in solventless systems*, 1996, Google Patents.
- [30] Teng, H., Overview of the Development of the Fluoropolymer Industry. Applied Sciences, 2012. 2(2): p. 496-512.

- [31] Velez-Herrera, P. and Ishida, H., Synthesis and characterization of highly fluorinated diamines and benzoxazines derived therefrom. Journal of Fluorine Chemistry, 2009. 130(6): p. 573-580.
- [32] Choi, S., Lee, S., Jeon, J., An, J., Khan, S.B., Lee, S., Seo, J., and Han, H., A photoinitiator-free photosensitive polyimide with low dielectric constant. Journal of Applied Polymer Science, 2010. 117(5): p. 2937-2945.
- [33] Rogers, K. *Bisphenol A (BPA)*. 2014; Available from: <http://www.britannica.com/EBchecked/topic/681559/bisphenol-A-BPA>.
- [34] Schierow, L.J., Bisphenol A (BPA) in Plastics and Possible Human Health Effects. 2011: DIANE Publishing Company.
- [35] Organization, W.H., Toxicological and Health Aspects of Bisphenol A: Report of Joint Fao/Who Expert Meeting 2-5 November 2010 and Report of Stakeholder Meeting on Bisphenol a 1 November 2010 Ottawa, Canada. 2012: World Health Organization.
- [36] Md, A., Rasheed , Kola, R., Kumar , and Yalavarthy, P., Devi Assessment of Antibacterial Activity of Bisphenol A (4,4'-Isopropylidenebisphenol). International Journal of Innovative Research in Science, Engineering and Technology, 2013. 2(11): p. 6003-6008.
- [37] Sigma-Aldrich. *Material Safety Data Sheet : Bisphenol A*. Available from: <http://www.sigmaaldrich.com/catalog/product/aldrich/239658?lang=en®ion=SG>.
- [38] Chemical, H.O.F. *Bisphenol AF*. Available from: <http://www51.honeywell.com/sm/specialtychemicals/ofc/products-n2/bisphenol-af-n3/bisphenol-af.html?c=21>.
- [39] Sigma-Aldrich, 4,4'-(Hexafluoroisopropylidene)diphenol 2014.
- [40] Biotechnology, S.C. *4,4'-(Hexafluoroisopropylidene)diphenol (CAS 1478-61-1)*. 2014; Available from: <http://www.scbt.com/datasheet-262203-4-4-hexafluoroisopropylidenediphenol.html>.
- [41] Sheets, P.T.C.F. *Anthrax spore decontamination using paraformaldehyde* Available from:

- http://www.epa.gov/opp00001/factsheets/chemicals/paraformaldehyde_factsheet.htm.
- [42] Agency, U.S.E.P. *Formaldehyde*. 2000; Available from: <http://www.epa.gov/ttn/atw/hlthef/formalde.html>.
- [43] ChemicalBook. *Paraformaldehyde*. 2010; Available from: http://www.chemicalbook.com/ChemicalProductProperty_EN_CB5233205.htm.
- [44] Millipore, M. *104005 Paraformaldehyde* 2014; Available from: http://www.merckmillipore.com/thailand/chemicals/paraformaldehyde/MDA_CHEM-104005/thai/p_uE6b.s1L154AAAEWluEfVhTL.
- [45] Chemours, Uses & Applications. 2015.
- [46] Millipore, M. *822172 4-Aminobenzotrifluoride* 2014; Available from: http://www.merckmillipore.com/TH/en/product/4-Aminobenzotrifluoride.MDA_CHEM-822172.
- [47] Sigma-Aldrich. *4,4'-(Hexafluoroisopropylidene)diphthalic anhydride*. 2014; Available from: www.sigmaaldrich.com/catalog/product/aldrich/386448.
- [48] BASF. *N,N-Dimethylacetamide*. 2014; Available from: http://www.basf.com/group/corporate/en/brand/N_N_DIMETHYLACETAMIDE.
- [49] Labscan, R. *Dimethylacetamide, AR*. 2014; Available from: http://www.rcilabscan.com/modules/productview.php?product_id=1923.
- [50] Wang, C., Zhao, X., Li, G., and Jiang, J., Novel fluorinated polyimides derived from 9,9-bis(4-amino-3,5-difluorophenyl)fluorene and aromatic dianhydrides. *Polymer Degradation and Stability*, 2009. 94(10): p. 1746-1753.
- [51] Hsiao, S.-H., Guo, W., Chung, C.-L., and Chen, W.-T., Synthesis and characterization of novel fluorinated polyimides derived from 1,3-bis(4-amino-2-trifluoromethylphenoxy)naphthalene and aromatic dianhydrides. *European Polymer Journal*, 2010. 46(9): p. 1878-1890.
- [52] Mistry, B.D., *A Handbook of Spectroscopic Data: Chemistry - UV,IR,PMR,CNMR and Mass Spectroscopy*. 2009, India: Oxford Book company.

- [53] Tiptipakorn, S., Punuch, W., Okhawilai, M., and Rimdusit, S., Property enhancement of polybenzoxazine modified with monoanhydrides and dianhydrides. Journal of Polymer Research, 2015. 22(7): p. 1-11.
- [54] Wang, J., Wu, M.-q., Liu, W.-b., Yang, S.-w., Bai, J.-w., Ding, Q.-q., and Li, Y., Synthesis, curing behavior and thermal properties of fluorene containing benzoxazines. European Polymer Journal, 2010. 46(5): p. 1024-1031.
- [55] Rocks, J., Rintoul, L., Vohwinkel, F., and George, G., The kinetics and mechanism of cure of an amino-glycidyl epoxy resin by a co-anhydride as studied by FT-Raman spectroscopy. Polymer, 2004. 45(20): p. 6799-6811.
- [56] Santhosh Kumar, K.S., Reghunadhan Nair, C.P., and Ninan, K.N., Investigations on the cure chemistry and polymer properties of benzoxazine–cyanate ester blends. European Polymer Journal, 2009. 45(2): p. 494-502.
- [57] Nakamura, S. and Nishimoto, Y., Synthesis and Properties of Fluorine-containing Aromatic Condensation Polymers Obtained from Bisphenol AF and Its Derivatives, in Fluoropolymers 1: Synthesis, G. Hougham, et al., Editors. 2002, Springer US. p. 127-150.
- [58] DuPont. *Kapton HN*. 2015; Available from: <http://www.dupont.com/content/dam/dupont/products-and-services/membranes-and-films/polyimide-films/documents/DEC-Kapton-HN-datasheet.pdf>.
- [59] Velez-Herrera, P. Functional Polybenzoxazine Resin as Advanced Electronic Materials. Case Western Reserve University, 2008.
- [60] Krishnan, S., Kwark, Y.-J., and Ober, C.K., Fluorinated polymers: liquid crystalline properties and applications in lithography. The Chemical Record, 2004. 4(5): p. 315-330.
- [61] Enterprises, D. *Surface Energy Data for PTFE: Polytetrafluoroethylene*. 2015; Available from: www.accudynetest.com/polymer_surface_data/ptfe.pdf.

VITA

Mr. Patcharat Pattharasiriwong was born in Narathiwat Province, Thailand on September 10, 1990. He graduated at high school level in 2008 from Sarasit Phithayalai School, Ratchaburi, Thailand. In 2012, he received Bachelor's Degree in Chemical Engineering from the Department of Chemical Engineering, Faculty of Engineering, Srinakharinwirot University, Nakornnayok, Thailand. He continued study for Master's Degree of Chemical Engineering at the Department of Chemical Engineering, Faculty of Engineering, Chulalongkorn University, Bangkok, Thailand.

